esa BR-20

OCEAN COLOUR WORKING GROUP

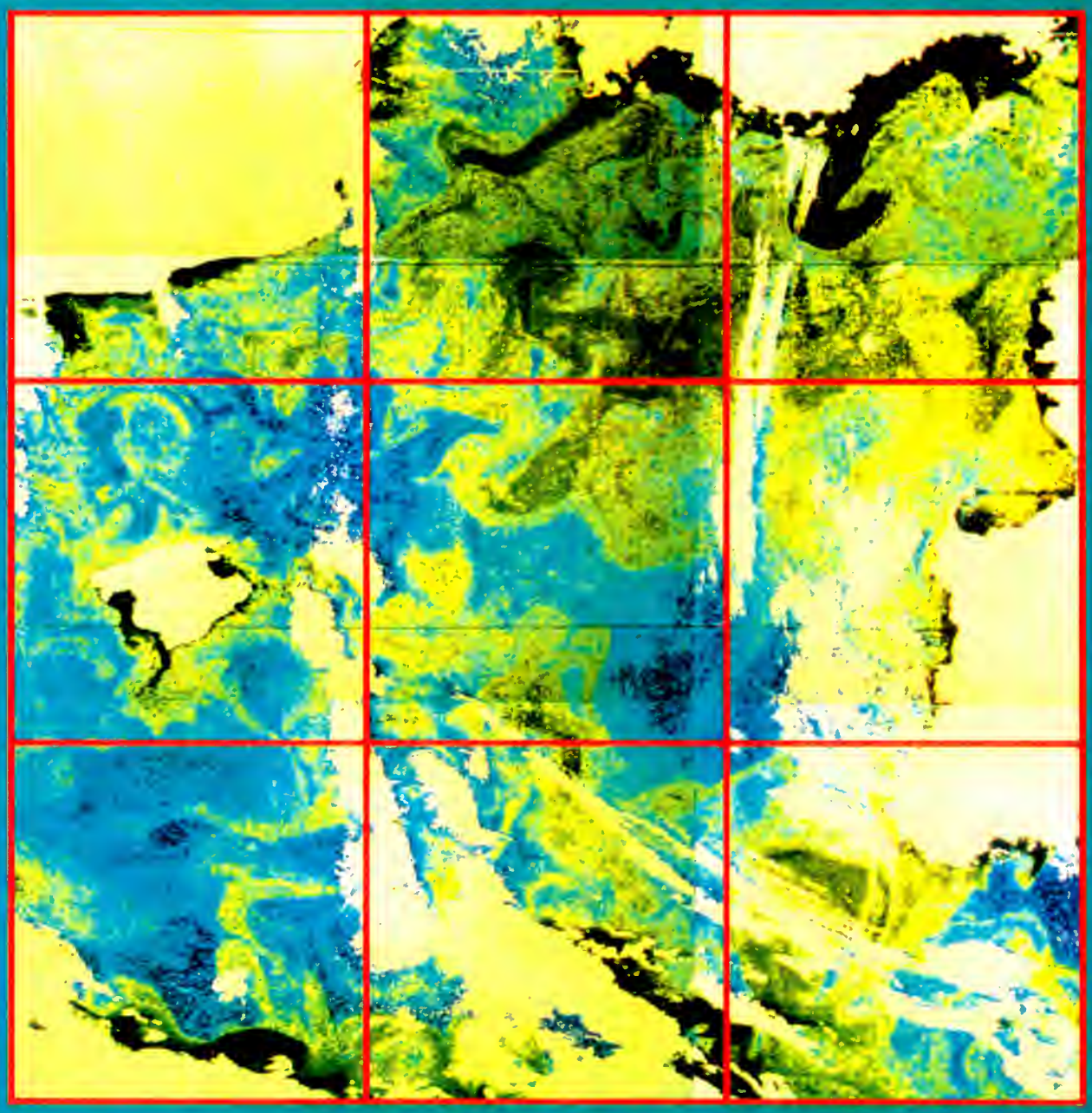

Progress report to

ESA Earth Observation Advisory Committee

June 1984

esa
european space agency
agence spatiale européenne

esa BR-20
June 1984

OCEAN COLOUR
WORKING GROUP

Progress report to

ESA Earth Observation
Advisory Committee

european space agency / agence spatiale européenne
8-10, rue Mario-Nikis, 75738 PARIS CEDEX 15, France

Cover picture

Nimbus-7 CZCS view of the Western Mediterranean Sea (24 *March* 1979; *orbit no* 2090).

Land and clouds are displayed in white and turbid areas in black. The atmospheric effect has been removed from the signals received by the sensor. The water-leaving radiances in the different channels are thereafter combined through algorithms to provide the chlorophyll (phytoplankton) concentration; from deep blue to dark green, the concentration varies from less than 0.07 *to more than* 0.16 mg/m^3.

This type of representation is of great interest in statistical studies of the primary production variation and also in monitoring the sediment transport from river plumes and coastal areas. In addition, this figure demonstrates how the turbulent field, the eddies and meanders of different scales can be visualised through the pigment concentration. The colour imagery, in the near future will most likely contribute a remarkable tool for the ocean dynamics studies.

ESA BR-20 Ocean Colour Working Group Progress Report 1983
ISSN: 0250-1589

Report prepared by the Ocean Colour Working Group of ESA Earth Observation Advisory Committee:
Prof. R. Frassetto (Italy), Dr. M. Reynolds (ESA), Prof. A. Morel (France),
Dr. H. van der Piepen (FRG), Dr. D. Spitzer (The Netherlands),
Dr. P.Y. Deschamps (France) & Dr. P. Holligan (UK) (newly appointed to the group).

Published by: ESA Scientific & Technical Publications Branch
ESTEC, Noordwijk, The Netherlands

Edited by: T.D. Guyenne & J. Hunt

Price Code: C1 (60 FF).

Contents

1. Introduction

At the 15th meeting of the Remote Sensing Programme Board (*ref. ESA/PB-RS/MIN/15*), the Executive was requested to investigate the possibility to maintain an option to fly an ocean colour monitoring (OCM) mission on ERS-2. Further, the Executive was requested to investigate an advanced OCM utilising electronic scanning techniques as opposed to mechanical scanning techniques used in the first OCM.

In accordance with this PB/RS request the Executive has undertaken a total of five actions, as follows:

- The definition of typical OCM interface requirements to enable the ERS-1 study contractors to identify the impact of an option to fly an OCM on ERS-2.
- The placement of three parallel industrial feasibility studies, to three separate industrial groups, to investigate to which extent electronic scanning techniques can fulfill the OCM multispectral imaging and photometric requirements. The three industrial groups are under the leadership of Matra, MBB and SNIAS.
- The placement of a further feasibility study, with the University College of London to investigate the potential application of Fabry-Perot interferometry with imaging photon detection techniques to ocean colour determination.

The results of all the above actions will be known by the end of 1983.

Furthermore, ESA Earth Observation Advisory Committee (EOAC) was invited to set up an Ocean Colour Working Group (OCWG) with specific tasks:

1. report on ocean colour ongoing and planned activities
2. identify updated technology of sensing the ocean colour for science and applications
3. identify further scientific investigations in the ocean colour and indicate needed experiments.
4. recommend further technological development.

EOAC charged Prof. R. Frassetto, member of EOAC, to set up the Working Group with Dr. M. Reynolds of ESA.

Four persons were selected to fill the required range of experience in marine and atmospheric optics, marine biology, atmospheric optics, and in the application of ocean colour in physical and biological oceanography, pollution monitoring and other experimental work, namely:

Prof.	A. Morel	(*France*)
Dr.	H. van der Piepen	(*FRG*)
Dr.	D. Spitzer	(*The Netherlands*)
Dr.	P.Y. Deschamps	(*France*)

Four meetings were held on 30 March, 18 May, 16 September and 22 November 1982 and a preliminary report was presented (ESA/OCWG (83)1) on June 3, 1983. After a meeting in November 1983, this report was approved for distribution.

The WG, in consideration of the fact that an OCM could be flown on ERS-2 only by 1990 or later, has recognised the need for ESA support of further technology and scientific research, and for a periodic (i.e. yearly) updating report to put the Executive in a condition to take proper decisions when the time occurs.

R. Frassetto, chairman of the WG, illustrated this point of view at the October '82 EOAC meeting and it was approved.

The present report summarises an updated state of the art in ocean colour physics, monitoring and use, and provides a first document to comply with the PBRS requests.

A second, updated report is proposed for 1986, which will contain information retrieved from the four ongoing contracts, from the SCOR WG 70*, from the Ocean Colour Science WG (OCSWG) of NASA** and from the experiments underway, some of them in international cooperation.

The 1986 report will attempt also to deal with the fine tuning of the channels, the frequency of information from a 3-day revisit satellite, considering the cloud coverage distribution per latitude, the better understanding of the fluorescence of the ocean and of its use in addition to the colour of the ocean, the potentials of combined colour, fluorescence, microwave sensing and finally a possible determination of standards for each parameter.

---

* *The SCOR WG 70 deals with general review of requirements of present and future capabilities of ocean remote sensing and of applications achieved and expected.*

** *The OCS WG was established in 1981 by NASA to deal mainly with utility of satellite ocean colour measurements, especially for measuring global ocean chlorophyll for studying the fate of global primary productivity in the sea.*

The general feeling of the WG is that the present configuration of the mechanical scanning OCM is the best compromise to provide the needed requisites for:

a. spectral resolution
b. spatial resolution
c. atmospheric correction
d. thermal imaging.

A brief clarification on the 800 to 1000 m spatial resolution is appropriate. It is felt that spectral resolution is more important than spatial resolution on a satellite considering the present limitations of data bit rate storage and ground processing. The short term phenomena which are dependent on estuarine outflows are transients and can therefore be better and more frequently surveyed by shore stations, ships and airborne sensing if they involve scales of the order of 10 km.

Remote sensing from satellite instead will monitor fruitfully the effects which involve coastal areas extending from 5 to 50 km and which have a time residence of more than 3 days. A simplified example of space and time domains of processes and sampling is shown in Figure 1.

The WG made a special effort to identify side products of an OCM which regard inland and climate applications.

The WG furthermore evaluated the benefits of the research and of the existing as well as of the future satellite system to monitor ocean colour. It was emphasised that CZCS of Nimbus 7 is degrading and is now being turned on, most of the time on US sites, and that ERS-2 could be the first chance to retrieve ocean colour data with advanced techniques and atmospheric correction after a period of satellite inactivity (1985–90?) particularly over European waters, unless Canada or Japan reconsider a colour sensing of the ocean before that date.

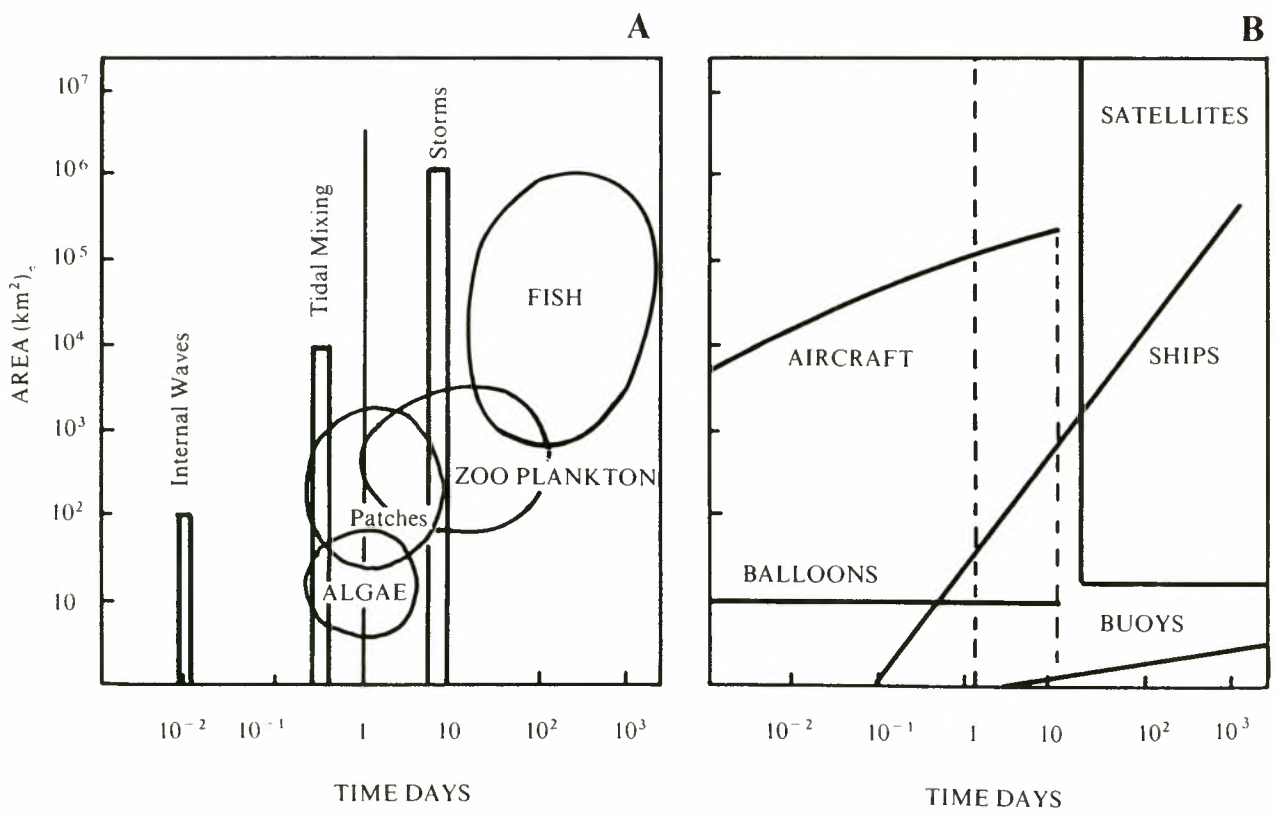

Figure 1. Simplified Space and Time Domains for Some Oceanic Processes and Sampling by means of different tools.

2. Ocean colour background

2.1 HISTORY OF WATER COLOUR RESEARCH

Optical oceanography and subsequently water colour research originates from ship measurements, laboratory work and theoretical studies. The activities of leading laboratories mainly in the USA, Japan and Europe, during the past decades, helped to establish the relationships between the 'apparent' optical properties of the sea, such as its spectral reflectance (which governs its colour), and the 'inherent' optical properties, such as absorption and scattering. In addition, the change in the inherent properties of a water body induced by the presence of the various substances (particulate and dissolved) has been investigated.

During the 1970–78 period, several important cruises were partly devoted to optical oceanography, often in relation to primary production studies.

The application of remote sensing techniques, however, added a new dimension to these activities. Data from low-flying aircraft were collected above the water and compared with sea truth from ship measurements. Soon the need for more specific instruments was realised. One of them, which was developed specifically for water colour research, was NASA's Ocean Colour Scanner (OCS) flown mostly on the U-2 aircraft above coastal waters of the US. The high altitude achieved by this special jet aircraft in simulation of space platforms stimulated work on the study of atmospheric effects on the colour signal. The U-2/OCS programme served as preparation for the Coastal Zone Colour Scanner (CZCS) on the Nimbus-7 satellite which is the first dedicated water colour sensor in space (launched in October 1978). The CZCS is considered as a major breakthrough in water colour research from space and associated applications. After the initial delay in the data distribution, it has produced many scenes of the world's oceans and coastal regions which are still processed and analysed in many laboratories around the world. As a consequence, studies in optical oceanography were simultaneously re-activated and post-launch calibration cruises were organised mainly with the aim of getting sea truth measurements.

As a by-product of this activity at sea, the bio-optical data bank has been considerably enriched, and can be used now in predictive studies for 'simulated' new sensors.

With the increased capability of some laboratories in processing CZCS data almost in real time, new and multipurpose researches (e.g., ODEX and Rings Experiments) have been recently conducted at sea. Such complementary satellite and ship data provide a spatial-temporal description of mesoscale ocean features with their dynamic, optical and biological implications.

2.2 PHYSICS OF OCEAN COLOUR

The spectral composition of the upwelling radiance ('the colour') above the sea is determined by:

a. the spectral composition of the downwelling solar irradiance
b. the inherent optical properties of the water column – absorption, scattering – and, in a minor way, by the fluorescence.

As summarised in Table 1, the inherent optical properties of a water body are determined by the inherent optical properties (absorption and scattering) of pure sea water and by those of the suspended and dissolved materials therein, namely the particulate organic matter (phytoplankton and by-products), the inorganic (re-)suspended particles and the dissolved organic decay products ('yellow substance') of mainly terrestrial origin. These properties are rigorously additive (1)*, so that the absorption coefficient of the water can be expressed as the sum of the partial absorptions:

$$a = a_w + \sum_{1}^{n} a_x^* \{x\}$$

where a_w is the absorption coefficient of the sea water (at the wavelength considered), a_x^* is the specific absorption coefficient for a given constituent X (specific = per unit of concentration) and $\{x\}$ is the concentration of that constituent.

The corresponding expressions for b (the scattering coefficient) or for b_b (the back scattering coefficient) can be written in the same way.

The theoretical description of an apparent property, such as the upwelled radiation, and of its link with the inherent properties, is based upon the treatment of the radiative transfer equation with appropriate boundary conditions. The radiance which emerges from the ocean is directly governed by the reflectance, R (or irradiance ratio, i.e. the ratio of upwelling to downwelling irradiances at the zero level). Various approaches and

* *Numbers between parentheses refer to the bibliography in Chapter 8.*

Table 1

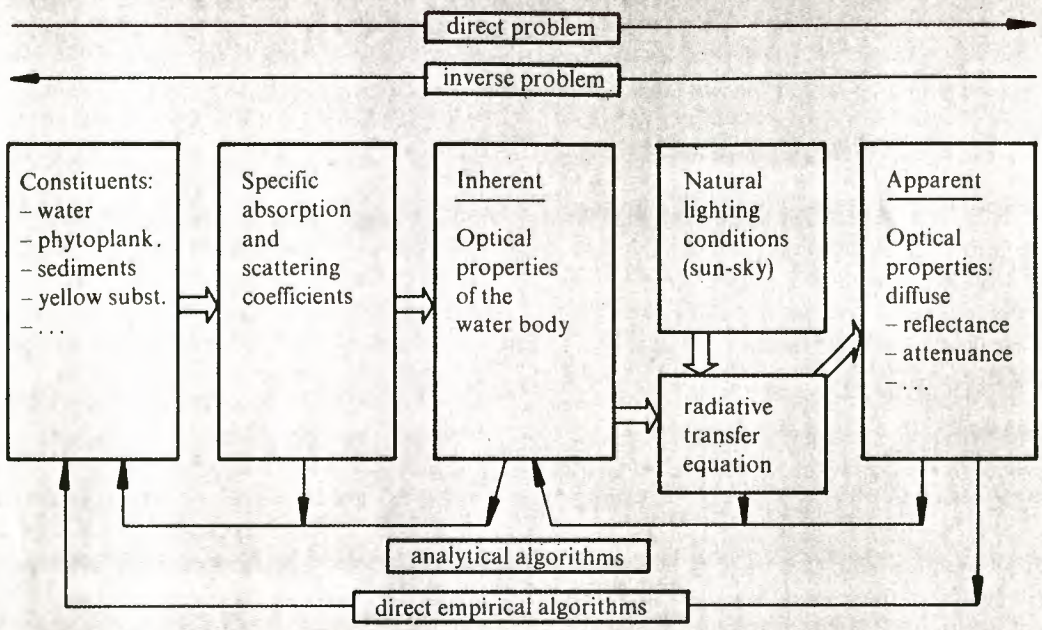

solutions of the radiative transfer problem are available (2,3,4), which demonstrate that R (in a first approximation) is simply proportional to b_b/a or $b_b/(a+b_b)$. Such a relationship, combined with the knowledge of the specific optical coefficients, allows in principle the concentrations of diverse substances to be inferred from R, provided that a sufficient number of equations can be written (one per wavelength).

The 'analytical algorithms' would correspond to this approach (5). This approach is conditioned by a sufficient knowledge of the optical properties of each intervening component. Some progress has been made concerning the yellow substance absorption (6,7,43) and the optics of the algal cells (8,9,44). The specific optical properties of inorganic suspended matter, likely more variable, are less known and not adequately quantified.

Direct relationships have been established between the spectral reflectance values and the concentrations through statistical analyses (10,11,12,13). Once they have been inverted, these relationships form the 'empirical algorithms'. For the CZCS data processing, and due to the limitation of this sensor (number of channels), these algorithms are the only ones which can be practically used. With an increase number of channels and an improved radiometric sensitivity, it can be expected that not only the analytical approach will be possible, but also more powerful statistical treatment could be used (eigen vector method, for instance, which would allow a separate assessment of several constituents to be achieved (25)).

Another important physical aspect of the ocean colour has been investigated and deals with the 'penetration depth'. The upwelling radiance is due to photons backscattered from different levels beneath the surface which carry information from different layers. It has been shown (14) that for a homogeneous ocean, the depth above which 90% of the backscattered radiation originated is the inverse of the irradiance attenuation coefficient, K. A sensor 'looks' into the water and collects information from a layer the thickness of which is $Z_p = 1/K$, hence called 'penetration depth'. This thickness depends on the optical transparency of the water and, for a given water, depends on the wavelength. It may range from less than 1 m to approximately 30 m (see Chapter 7, Fig. 9).

The colour (reflectance) of a vertically inhomogeneous water is governed by weighted concentrations within the same layer, the weighting function depends on the vertical distribution of the substances through the attenuation coefficient, also variable with the depth (15). If the direct problem can be solved, the inversion leads to multiple solutions.

Another phenomenon has been recognised inside the signal emerging from the sea, i.e. the natural chlorophyll fluorescence which is excited by the solar radiation

(26,27,28). The emission, centered around 685 nm ($\simeq$ 20 nm wide), is specific and quasi-insensitive to the presence of other substances (except a high amount of yellow substance which would reduce the exciting blue radiation). As the water is highly absorbing in the red, the emitted light is quickly re-absorbed and thus only superficial (1–2 m) phytoplankton is detectable. The relationships between the intensity of the fluorescence and the concentration in chlorophyll *a* have been found very variable (see e.g. 29). The pigment is inside the algal cells (in chloroplast) and the fluorescence response depends upon the species and its inner and external wall structure. For a given species, the response is also affected by the physiological, nutritional and environmental (light) conditions. Independent determination of the algal biomass concentration and its ability to fluoresce are of interest, since the nonlinearity of the emission vis-à-vis the concentration is, for biologists, an index in physiological studies.

Unfortunately, the radiance emerging from the sea undergoes some alterations when travelling through the atmosphere before reaching the satellite sensor. Besides this perturbating effect, a considerable amount of photons scattered by the air molecules and aerosols, or reflected at the interface (or both) are added to the initial marine signal (it is assumed that the sun glint is outside the field of view of the detector). Typically the marine signal forms at the most 20% of the total signal received by the sensor and may vanish in the atmospheric noise in bad conditions (and at unfavourable wavelengths). This rather uncomfortable situation emphasises the need for accurate 'atmospheric corrections' to recover the marine information (see Chapter 2.3).

In conclusion, the physics of ocean colour remote sensing is well understood and the problems accurately identified, even if they are not completely solved (17).

This basic research has proved its usefulness for a comprehensive interpretation of the CZCS imagery, while not being fully exploited due to the limitations and constraints imposed by this specific sensor. Future improved sensors will take advantage more efficiently of this fundamental work.

2.3 MODELLING AND CORRECTION OF ATMOSPHERE AND SURFACE REFLECTION EFFECTS

Both the atmosphere and the sea surface produce a noise effect on the signal to be retrieved from the subsurface which can be summarised as follows:

a. Absorption by the atmospheric gases
b. Scattering by the molecules of the atmosphere.
c. Scattering by the particles of the atmosphere.
d. Specular reflection of diffuse solar radiation (sky radiance) on the wavy water surface (sky glint).
e. Specular reflection of direct solar radiation on the wavy water surface (glitter or sun glint).
f. Diffuse reflection on sea foam covering partially the water surface.

The first three effects (a,b,c) refer only to atmospheric processes; the other ones (d,e,f) refer to surface reflection with some interaction with atmospheric processes (d,e).

The objective of the OCM should be to consider these phenomena as signals for applications in climate research and as noise to be corrected for ocean colour sensing. A description is given of each of these phenomena.

a. Absorption by the atmospheric gases
Absorption by gases can be accurately modelled and corrected for, if the total (vertically integrated) contents of the absorbing gases are known. This is the case for CO_2 and O_2. O_3 and H_2O are variable with time and location, but their effect is small, provided that the sensor channels are correctly selected in atmospheric windows: their residual influence can then be corrected for by assuming a climatic mean value of the total contents of these two gases. This does not request any additional channels to the experiment, or in situ measurements.

b. Molecular (Rayleigh) scattering of the atmosphere
The effect is large and increases rapidly towards the shorter wavelengths:
- increase of the mean reflectance ($\simeq$ 0.15 reflectance at $\lambda = 400$ nm) with large polarisation;
- loss of sensitivity to the variations of the water body reflectance due to the diffuse transmittance between the sun and the surface and to the direct transmittance between the surface and the sensor ($\simeq$ 0.5 transmittance at $\lambda = 400$ nm, 60° solar zenith angle, nadir viewing);
- background or adjacent effects: the measured signal is a mixing of the signals coming from the observed target (80% at $\lambda = 400$ nm) and from its background (20%).

Those effects can be calculated easily from the geometric conditions without other data, but they rely on an accurate absolute calibration of the sensor versus the solar constant, and on a precise knowledge of the polarisation of the sensor optics.

The calibration problem was encountered and gave problems on the present CZCS experiment.

c. Scattering by particles (aerosols under clear sky conditions.
The aerosol scattering produces the same effects as does molecular scattering, but:
- the increase of the mean reflectance is variable with the aerosol loading (aerosol type, particle size distribution, concentration number) with location and time; and
- transmittance and background effects are small and do not require accurate corrections.

The proposed atmospheric correction methods to eliminate this variable aerosol influence are all based on the hypothesis that the spectral behaviour of the optical aerosol properties is rather regular. This spectral behaviour can be observed at wavelengths where the water body is 'black' (e.g. $\lambda > 0.7\ \mu m$), or if its reflectance is known (e.g. $\lambda > 0.5\ \mu m$ for 'clear water').

Extrapolation or interpolation is then to be done at other wavelengths. An accurate determination of the aerosol spectral behaviour requires additional channels in the infrared up to 1 μm, or even 1.6 μm for some aerosol types. The CZCS experiment missed an accurate determination of the atmospheric correction because observations were limited to 0.67 μm. The OCE experiment on-board OSTA-1 has channels extended to the near infrared, allowing better extrapolation and aerosol correction.

d. Specular reflection of the diffuse sky radiance on the water surface (sky glint)
This term includes radiation scattered by molecules and aerosols towards the water surface and then specularly reflected. It may be calculated (for molecular scattering) and corrected for aerosol scattering) in a similar way to the above sections b and c.

e. Specular reflection of the direct solar radiation on the water surface (sun glint or glitter)
This term depends strongly on the sea surface state (local wind stress and swell), through the probability to find elements of the wavy surface having the particular slope permitting specular reflection of the direct solar radiation towards the sensor. This glitter component has a spectral behaviour close to the aerosol scattering component and is thus mostly removed by the extrapolation/interpolation procedure for the correction of aerosols.

The accuracy of the glitter correction is limited at high levels of glitter, by:
- the accuracy of the interband relative calibration of the sensor
- the interaction between glitter and molecular scattering at shorter wavelengths (400–450 nm) which may require an independent determination of the glitter value at 2.2 or 3.7 μm.

By a tilting capability of the sensor, more or less like the CZCS included (20° tilting off nadir), high glitter values can be avoided. But tilting increases the complications of the mechanical scanning and geometrical corrections, hence weight and costs. However, it is generally felt that data without tilting are largely usable: simulation of the process shows that less than 1/3 of the usage is highly contaminated and unusable in the most severe cases, probably very much less as a mean value.

f. Sea foam reflectance
The percentage of the sea surface covered by sea foam increases with wind speed. The result is an increasing diffuse reflectance of the surface. This effect is corrected for by the correction procedure for aerosol scattering as long as the sea foam reflectance has a spectral behaviour close to the aerosol scattering. This is supported only by the visual appreciation that sea foam is 'white'.

2.4 TOOLS, METHODS AND INTERPRETATION OF DATA

The variety of biological patterns in the ocean and their driving mechanisms are spread in different scales and need different tools to be surveyed and described. Table 2 gives an approaching classification to the problem.

The upwelling and downwelling (ir)radiance can be measured in situ by submersible spectral instruments. Remote sensing measurements from aircraft or satellites involve the application of spectral radiometers (good spectral resolution, poor spatial resolution) and of multispectral scanners (good spatial resolution in several specific spectral bands). Design of the multispectral scanners requires availability of thorough knowledge on the nature of the relationships between the ocean colour and the sea truth, so called ocean colour algorithms. The results yielded from the marine-optical research and from experiments employing airborne or shipborne spectral radiometers can be used for specifications of the optical design (position of the spectral bands and their width) of the satelliteborne instruments.

In the application of remote sensing to open ocean and

Table 2. Scaled biological patterns in the ocean, their driving mechanisms and measuring tools.

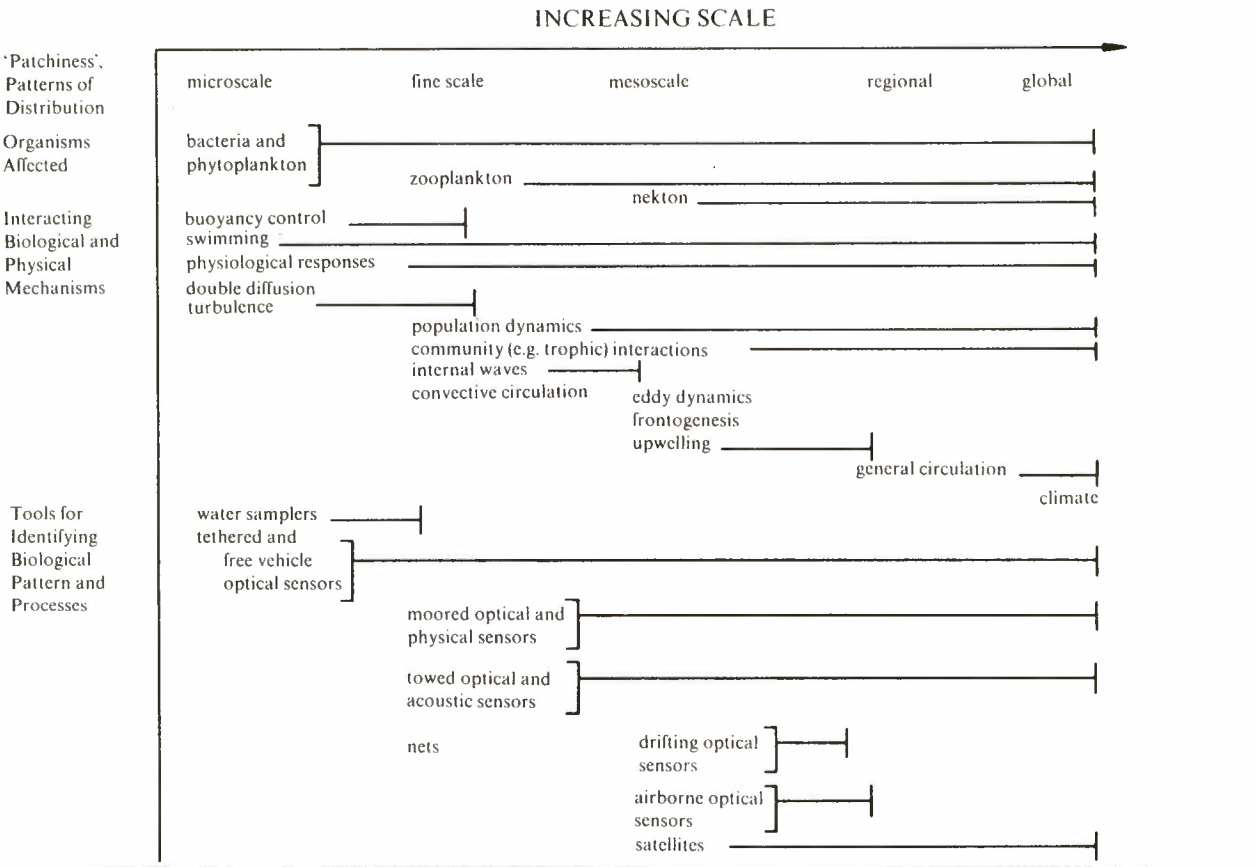

(reproduced from MAREX document)

coastal areas, the present knowledge shows the necessity to distinguish between different types of water and Morel's classification could be adopted as a first approach. This classification, as summarised by Table 3 (from H.R. Gordon & A. Morel (17)), considers two cases:

Case 1 waters are those for which phytoplankton and their derivative products play a dominant role in determining the optical properties of the ocean, and thus its 'colour'.

The derivative products are both particulate debris and dissolved yellow organic matter (of weak influence), (components 1, 2, 3, Table 3).

As a rule, *oceanic waters* form the Case 1 waters; these waters, however, may be present even in coastal zones in absence of continental shelf and of terrigenous influx.

Case 1 waters range from oligotrophic – and deep blue waters (with chlorophyl lower than, say, 0.1 mg/m^3) to moderately productive green waters ($C \simeq 1$ mg/m^3) and even to some eutrophic – and dark green waters (with $C \simeq 10$ mg/m^3) which can be encountered in upwelling regions along arid coasts.

Case 2 waters are those waters which may or may not, contain the components 1, 2 and 3. Waters depart from Case 1 to enter into Case 2 because of:

(i) their high sediment load (*influence of* 4 *and* 5) as they are 'sediment-dominated Case 2' waters;
ii) their high terrigenous yellow substance content (component 6); they are then 'yellow-substance-dominated Case 2' waters, if the turbidity remains low; and
iii) their cumulated influences.

In addition, human and industrial activities can also generate Case 2 waters, or superimpose their effects on existing coastal Case 2 waters. Case 2 waters of diverse kinds are normally encountered in *coastal areas* (estuaries, shallow waters, inlets, etc.) and possibly far from the coastline above the extended *shelves or banks*. Likely Case 2 waters form less than 5% of the world oceans, but they are important to monitor.

Some (nonlinear) co-variations of the optical properties of Case 1 waters with chlorophyll *a* content have been observed and allow a meaningful interpretation of the sensed colour to be given. Case 2 waters are by definition more unpredictable. The interpretation of their colour is more complex and a higher number of channels is required to discriminate between and separately assess the different components. These questions are examined below in detail.

MINIMUM NUMBER OF CHANNELS FOR CASE 1 WATERS

At the present state of knowledge, one parameter is sufficient for the *bio-optical classification of the water* which, can be expressed in terms of chlorophyll *a* concentration or total seston concentration (*C* and *S* respectively). This situation results from the co-variations above mentioned.

The detection of the bio-optical state is based on the value of the 'blue to green ratio', i.e. for CZCS

$Lu\,443/Lu\,550$*

or $Lu\,520/Lu\,550$

The second ratio is used, while less sensitive than the first one, when the signal $Lu\,443$ is too low to be restored (after atmospheric corrections) with a sufficient accuracy, in the case of high chlorophyll *a*. Note that the red channel at 670 nm is also needed for the estimation of the aerosol content; the need for red and IR channels to effect the atmospheric corrections has been examined separately in Chapter 2.3.

MINIMUM NUMBER OF CHANNELS FOR CASE 2 WATERS

The problem addressed is to discriminate between and to separately assess:

- the particles with chlorophyll (*C*, as in Case 1 waters)
- the particles without chlorophyll, *X* ('turbidity')
- the yellow substance content, *Y*.

* *Lu means the upwelling radiance just above the surface.*

Table 3. Water classification in two cases with 7 components.

CASE 1 WATERS
1. LIVING ALGAL CELLS variable concentration
2. ASSOCIATE DEBRIS originating from grazing by zooplankton and natural decay
3. DISSOLVED ORGANIC MATTER liberated by algae and their debris (endogeneous yellow substance)
CASE 2 WATERS
4. RESUSPENDED SEDIMENTS from bottom along the coastline and in shallow areas
5. TERRIGENOUS PARTICLES river and glacial runoff
6. DISSOLVED ORGANIC MATTER land drainage (terrigenous 'yellow substance')
7. ANTHROPOGENIC INFLUX particulate and dissolved materials

Summarising a study using an eigenvector analysis (25), the conclusions at the current state-of-the-art are as follows (they do not prejudge the results of further studies and improvements among the scientific community):

1. The first vector (responsible for >96% of variance) is highly correlated with *X* meaning that this component is the most easily and accurately detected parameter.
2. With $C < 1$ mg/m^3, the chlorophyll signature appears unrecoverable in the presence of unknown amounts of *X* and/or *Y*; with $C > 1$ mg/m^3, the chlorophyll signal can be retrieved even in the presence of high *X* or *Y* values. The *Y* concentration, however, remains hardly recoverable.
3. The vectors are better correlated with *Y* if $C < 1$ and *Y* becomes detectable. In any case, correlation coefficients are less significant for *Y* than for *C* or *X*.

These conclusions rest on the assumption that the reflectance spectrum is known with accuracy at 27 wavelengths (i.e. between 400 to 650 nm at 10 nm intervals and at 700 nm, with the fluorescence peak region being left out). When considering a more restricted number of channels:

1. The OCM group (400, 445, 520, 565, 640 nm) appears to be the most efficient, almost as efficient as the 27 wavelength group in parameters retrieval.
2. If the wavelength domain 400 – 440 (i.e. the first OCM channel) is dropped out, a drastic decrease in the capacity of discriminating C from Y and of retrieving C or Y would result. The retrieval of X instead would remain practically unaffected.

ADDITIONAL CHANNEL(S) FOR THE FLUORESCENCE PEAK (685 NM)

Both Case 1 and Case 2 waters are concerned. However, waters with $C < 0.5\ mg/m^3$ ($> 90\%$ of the world's oceans) appear to be outside the capability of this technique owing to the weakness of the fluorescence efficiency. The measurement involves at least 3 channels: one is centered on the peak and two on either side of it, to establish a baseline.

The *in situ* emission is centered around 685 nm (20 nm wide); a narrow oxygen band at 688 nm shifts the apparent maximum if seen through the atmosphere. Also the nature of the fluorescent algae and the presence of other suspended and dissolved materials can cause shifts of the maximum from about 680 nm to 695 nm. Gower and Borstad (34) have proposed that the peak be consequently measured at 675 nm and the baseline be established through measurements at 650 and 750 nm. With the broad water bands (723 – 732 nm) and the narrow intense O_2 band at 762 nm, a delicate choice has to be made. The expected OCM configuration in this spectral domain (640, 685, 785 nm) is likely to be a good compromise.

3. Applications and merits

In the following chapters, the potential applications of water colour monitoring are briefly outlined. The various applications include monitoring in:

- lakes and rivers
- estuaries and tidal flats
- coastal zones
- enclosed/semi-enclosed seas
- open ocean areas
- polar regions
- ice-sea interface

and thus address a large variety of experimenters/users who are active in relevant fields:

- marine biology and ecology at global, regional and local scales
- coastal processes and monitoring
- ocean dynamics (global, regional and local scales)
- climate research
- fisheries
- inland areas
- pollution monitoring.

3.1 MARINE BIOLOGY AND ECOLOGY AT GLOBAL, REGIONAL AND LOCAL SCALES

The marine photosynthesis process, through which the organic matter forming the phytoplanktonic biomass is created, has several impacts on the marine biosphere, on the atmosphere and on the lithosphere.

The radiant energy received by the ocean is mainly converted into heat. A small part (10^{-4} to 10^{-2}) however is transformed into chemical energy by photosynthesis, and forms the energetic influx for the entire marine biosphere; all life in the sea originates from the algal biomass which is the first link in the entire food chain, from the bacteria to the fishes and mammals, and from the surface to the bottom.

With regard to the atmosphere, the marine primary production, estimated between 30 to 50% of the global primary production (18), results in a (transitory) storage of photosynthetically fixed carbon. The rate of the CO_2 fixation depends on the biomass present and also its ability to grow (productivity). The algal growth rate is light-controlled and nutrient limited. Among the necessary nutrients (N,P,Si, + oligoelements), nitrogen is crucial so that the fate of carbon and nitrogen are interrelated. Note that for both CO_2 and N, impact of human activity can no longer be considered as negligible when compared to natural processes.

With regard to the lithosphere, the marine biological activity, by generating detritus contributes to sedimentation in proportions which vary according to the importance of the terrigenous influx (and consequently of the land distance). As far as a complete oxidation of the settling materials is not accomplished, the organic carbon deposit constitutes a biotic sink for CO_2. This sink is likely more efficient in the vicinity of shelves and continental slopes (19).

The pigment (chlorophyll) concentrations are a convenient index of the phytoplanktonic biomass and at the present time, can be measured from space with reasonable accuracy, which will likely be improved in the near future. An assessment of the algal biomass and possibly of the primary productivity at a global scale form an important goal. As a matter of fact, ocean productivity and CO_2 fixation have recently been highly controversial and generally it is believed to have been drastically underestimated (20,21) in oligotrophic waters and, to a lesser extent, in eutrophic coastal waters. For obvious reasons ship-bounded programmes cannot properly address this problem. The spatial and temporal coverage which is needed is only achievable from space, even if improvements of productivity models, in situ methodology, as well as repeated measurements at sea remain necessary. This knowledge is a keystone in the debate about the fisheries regulation and potential harvest; it is also a clue to the bio-geochemical carbon cycle and parent cycles.

The preceding objectives, even if they concern the world's oceans, imply studies which necessarily have to be made at the mesoscale. In spite of a low algae stock, the oligotrophic areas ($\sim 90\%$ of the world's oceans) are responsible for the major part of the primary production. A production mapping must be able to distinguish the nuances in chlorophyll content which are associated with dynamical features at different scales, from the large ones (e.g. western boundary currents or equatorial currents), to intermediate ones (meanders, fronts, cores, eddies).

Moreover, the productive shelf zones, including the eutrophic coastal upwelling areas, exhibit complex dynamic, chemical and finally biological processes which typically belong to the mesoscale. The temporal variability and the areal extent of the permanent eastern upwelling systems are far from being known.

The zonal migration of these upwellings induced by trade winds (and monsoons), the start of blooms along the shelf breaks, the nature and the intensity of the biological response to meteorological events or impulses, are mesoscale phenomena which remain poorly

documented due to ship cruise limitations. Only repetitive coverage and synoptic views from space can adequately answer these questions (see e.g. 22,23). Not only colour imagery but also thermal imagery, insolation estimates from satellite data (24), wind stress field, etc. must be combined in a comprehensive study of the above mentioned phenomena. Chemical models of vertical mixing, thermocline, nutrients resupply, as well as biological-physical models of primary productivity, are also involved in this kind of study.

According to the spatial resolution achievable, the pigment distribution can be usefully studied down to small scales (< 0.5 km) and thus give partial access to the phytoplankton patchiness. At this local scale, other biological or ecological processes are accessible to remote colour measurements, such as the (natural) influence of estuarine outwelling upon algal production, and the (natural or anthropogenic) eutrophication, locally induced by an enhanced flux of nutrients.

In conclusion, mapping of chlorophyll at different scales but everywhere is an important tool for monitoring the health and abundance of marine life and any trends which may become detrimental or beneficial to mankind.

3.2 COASTAL PROCESSES AND MONITORING

Survey and monitoring of the coastal areas belong to the essential tasks of the coastal management agencies. Application of remote sensing (RS), when dealing with the problems of the coastal environment, is recently broadly acknowledged. Of particular interest is the use of the RS methods for observation of the (inter-correlated) processes like river discharge and erosion, sediment transport along the coast, pollution origin, discharge and tracking, transport of the natural ('yellow substance', chlorophyll) and artificial tracers (dyes), and plankton blooms.

For the diverse 'Case 2' (see Table 3) waters which prevail in coastal zones more thorough knowledge of the local conditions is required. There is an evident need for a development of a spectral reflectance model, an empirical or a statistical approach specifically directed to the RS of the turbid and diversely loaded coastal water. It might appear that no general algorithms do exist, due to the diversity of the coastal aquatic conditions. Temporal and spatial dependence of the RS sea truth relationships must be investigated in order to specify the parameters supporting and supplementing the satellite data.

Since the spectral shape and the absolute values in the blue-green part of the reflectance spectra are dominated by the optical properties of the sediment and dissolved organic matter (generally non-covarying with chlorophyll), RS measurements at the chlorophyll fluorescence band (685 nm) might be important in the coastal waters. Though one must consider the uncertainties connected with the fluorescence method.

The above considerations point out that the coastal applications of the satellite measurements put rather stringent requirements on the specifications of the ocean colour instrument, though attainable within the framework of the studied (OCM) designs. The repetition of 2–4 days is suitable for observation of longer term processes (blooms, larger scale transport, land drainage), it is unsuitable for observations of the short term fluctuations connected e.g. with the tidal dynamics.

Considering the current achievements in the remote measurements of the concentrations of the suspended and dissolved natural materials in water, with respect to coastal processes analysis and monitoring, it appears that:

1. Chlorophyll (total pigment) content can be retrieved from the 445/520 nm or 520/565 nm ratios with lower accuracy in the coastal waters than in the open ocean, due to the masking effects of sediments (30,31). Detection of the fluorescence effects of chlorophyll around 685 nm combined with the knowledge of the local sea truth conditions appears to be an attractive alternative.
2. Total suspended matter concentration can be determined using the 520/640 ratio (31).
3. No satisfactory algorithm for determination of the dissolved organic matter ('yellow substance') is available yet. Again, current investigations (32,33) on this subject should be continued and extended in order to make a substantial amount of (local) data available for a (more general) analysis.
4. Water pollution can be monitored either directly or through indirect effects. The tracking of the dumping sites and the control of the dispersion of the waste products is possible through the associated changes in the water colour.
5. If the glitter part of the upwelling signal can be separated from the water-leaving radiance, the oil contamination of the sea surface could be remotely measured by passive optical techniques.
6. The concentrations of heavy metals compounds and organic pollutants of terrestial origin seem to be correlated with the concentration of the terrigenous yellow substance and/or of the sediment load. The

compounds are often attached to the suspended particles. Knowledge of these rather complex relationships could enable the RS of the in-water-dissolved chemical pollutants.

3.3 OCEAN DYNAMICS

It is generally known that dynamic features in the oceans may, to some extent, be detected by the associated changes of sea surface temperature. This applies especially to large scale features like e.g. western boundary currents, warm or cold core rings as associated with the Gulf Stream meandering. Because different types of water are involved, most of these features are associated as well with a respective change of water colour. Early space photography but especially the more recent analysis of dedicated instruments like the CZCS on Nimbus-7 or the OCE on OSTA-I show these effects very clearly.

Independently of the achievable accuracy of pigment (or sediment) determination, and because phytoplankton and more generally seston can be considered as passive tracers, a visualisation of dynamic structures is possible through visible imagery. Present imagery (CZCS) has revealed its potential in describing the fluctuating mesoscale features such as meanders, fronts, and eddies of different scales. With the possibility of imaging the same area over a period of several days and weeks, and if patches have been clearly identified through their optical properties, then the trajectories of these patches can be delineated and used as the Langrangian approach in the circulation study. The colour imagery will likely constitute a reliable tool for the spatial and temporal description of these structures, as a byproduct. As emphasised before, these objectives cannot be separated from those pertaining to marine biology or, at least, results in both fields are complementary in the frame of a complete oceanographic study.

The ability of a colour sensor to visualise the marine structures originates from the fact that such a sensor 'looks' into the sea (down to 1 attenuation length) and thus can distinguish between water masses, hardly differentiated by the 'skin' properties in the infrared (or microwave) regions of the spectrum.

The radiometric temperature can be representative of the surface layer temperature (especially when vertical mixing takes place) but, in many occasions it is affected by interface perturbing influences (evaporation, diurnal warming, etc.) and no longer reflects the subsurface temperature. In that sense, colour and temperature imageries are not redundant and colour imagery could often prove its superiority in differentiating water masses. It is especially true at mesoscale; large scale structures, as Gulf Stream for instance, obviously exhibit both thermal and colour signatures, even if detailed studies show that colour aand thermal fronts may be horizontally non coincident and display different morphology in their fine structures (35). Cross-front diffusion could be at the origin of such a displacement.

Other examples of non-redundancy can be sighted. For example:

- coastal upwelling systems (such as Peru, Mauritania) show oscillatory characteristics due to the tradewinds. The newly upwelled and cold water is easily revealed by its thermal signature. After having drifted seaward, and being warmed up, this water becomes stabilised and productive, gains a colour signature whereas the thermal signature vanishes.
- small ($\sim$ 10–20 km) mesoscale structures, with marked density gradients (baroclinicity) are the seat of active circulations. Such a gradient can result (see Fig. 2 from ref. 42) from a salinity gradient without significant change in temperature. Thus the active zone is not detected by thermal imagery. On the opposite the isopycnal zone is sensed since a temperature gradient exists (which is compensated for by a reverse salinity gradient).

3.4 CLIMATE RESEARCH

3.4.1 *CARBON CYCLE OF THE SEA*

The carbon cycle of the sea, in particular its capacity for the storage of atmospheric carbon dioxide is very closely linked to the amount and fate of the annual marine primary production (marine carbon fixation). Estimates of the annual marine primary production range from 20 to 55×10^9 tons of fixed carbon per year (Ryther 1969; Platt 1975; De Vooys 1979; Walsh 1981). Uncertainties in these estimates arise especially from the strong spatial and temporal variability of the biomass in the highly productive shelf and upwelling regions, and from methodology in the oligotrophic open ocean (see Table 4).

Global mapping of chlorophyll and associated pigment concentrations at a suitable coverage and repetition rate could be used as an essential input for the modelling of primary productivity and its influence on the global carbon cycle.

3.4.2 *ENERGY TRANSFER*

Climate research depends to a large extent on suitable

Table 4. Uncertainty of carbon fixation within the sea (after Ryther 1969)

Province	Percentage of ocean	Area (10^6 km^2)	Mean productivity (gm C/m^2)/yr	Approx. range of chl. conc. mg/m^3	Total productivity 10^9 tons C/yr	(%)	Degree to which actual production may exceed reported values
Open ocean	90.00	326	50	0.01–0.1	16.3	(82)	$\leqslant \times 3 - \times 10$
Coastal zone	9.83	36	100	0.1–1.0	3.6	(18)	$\leqslant \times 3$
Upwelling areas	0.17	0.6	300	1.0–10.0	0.18	(0.5)	$\leqslant \times 2 - \times 5$
Total		362.6			20	(100)	

(reprinted from OCS WG, NASA, December 1982).

models for the energy transfer and exchange at the ocean/atmosphere boundary. The validation of respective models requires on a global scale input data on the heat storage and radiative transfer characteristics of solar radiation in both, the atmosphere and the oceans.

Heat storage by the sea
Solar radiation penetrating the surface layer is absorbed and converted directly into heat (a fraction is used for photosynthesis). The in-depth heating rates in the upper layers depend on the water optical properties resulting in different buoyancy and in different stratifications. This is especially important for the modelling and/or prediction of the thermocline and of the bulk surface temperature used in air-sea interactions, affecting thus both the regional climate and the heat transfer into the polar regions.

Furthermore, recent studies show that the daily temperature rise by solar heating below the mixed layer of the ocean is more sensitive to sea water turbidity than to cloud cover. Climatology of solar heating will become possible when global data of the seasonal variation of cloud cover and seawater turbidity are available (49).

Water optical properties (absorption and scattering) can be applied to the study of heat storage in the sea, e.g. a diffuse attenuation coefficient, k (absorption + back-scattering) derived from the CZCS data has been used for this purpose.

Because of the better capability of OCM to discriminate absorption and scattering properties, a much better determination of the heating rates in the ocean surface layer can be expected from OCM monitoring.

Aerosols and clouds
Although not dedicated for this purpose, a suitable ocean colour scanner (OCM) could support investigations into physical aspects of cloud and aerosol distribution and formation which are briefly outlined:

- The average cloud cover on a global scale is estimated in the order of 50%, however, tremendous variations of this factor occur on a regional and temporal basis. The capability of a sensitive ocean colour scanner to detect clouds (from cumulus to high level cirrus) is well-established and could support the highly needed investigations into cloud cover statistics.
- By combining visible/near infrared with imagery in the thermal infrared (especially with split windows), the cloud temperature and – through suitable models – the cloud top altitude may be determined. (This requires the range of the thermal channels to extend as low as 200 K!). This helps to distinguish between different types of clouds.
- Because of the different absorption properties of the liquid water and ice, by the aid of a suitable observation channel (1600 to 2200 nm) it is possible to distinguish between ice and water clouds.
- Under clear sky, the earth's radiation budget is influenced by the aerosol loading of the atmosphere, especially over the oceans. Because of the need for ocean colour measurements of precise atmospheric corrections, an aerosol loading product can also be derived from the experiment, such as the aerosol derived product from the limited wavelength range of the CZCS. A better aerosol loading product will be possible using the OCM with its wider range of channels, especially in the near infrared, which allows to determine the wavelength dependence of aerosol scattering and to relate it to the aerosol size distribution.

Surface albedo
The earth's radiation budget is also a function of the surface albedo. The well-calibrated OCM channels nearly cover the whole solar energy spectrum through the existing atmospheric windows. They can thus provide an accurate determination of the surface/albedo and of its spectral variations for climate research, but

also to study the associated changes of climate and vegetation (see 3.6).

Ocean circulation (global and regional)
The intermediate storage and the transport of heat (basically from the equatorial to the polar regions) is accomplished by the rather complex system of the major ocean currents. The remote assessment of ocean dynamic features has been accomplished by means of SST measurements, satellite altimetry and drifter buoys. However, since the evaluation of CZCS data, the water colour has been of great help in representing synoptically several marine features of the ocean.

3.5 FISHERIES CHARTS – EXPERIMENTAL PROGRAMMES

Investigators in the US are still learning how orbital remote sensing of the oceans can be useful and beneficial to commercial fisheries.

In an attempt to expand satellite technology from government-sponsored research to private-sector support and refinement for industrial use, a 'fisheries demonstration programme' is being carried out by NASA/JPL and commercial users of the US West Coast, with the participation and assistance of NOAA (NWS and NESS), the Navy/FNOC, USCG and Scripps Institution of Oceanography's Visibility Laboratory and Remote Sensing Facility.

This experimental programme is a research/technology transfer effort which provides a number of fisheries-aid analysis and forecast products to the US West Coast fishing industry, prepared with the aid of satellite observations of the ocean surface. Ocean colour boundaries derived from the Nimbus-7 CZCS are being merged with conventional and other satellite observations to form charts depicting key environmental properties that may contribute to more efficient fishing operations.

In particular, the experimental products for the programme are 'fisheries charts' (see Figs. 8 and 9 of chapter 7) depicting colour boundaries, key isoterms for selected fish species, convergence and upwelling areas (wind derivatives) mixed layer depths. These charts are generated on a daily basis, whenever useful satellite data can be received, and broadcast by single-sideband-radio-facsimile to commercial fishing vessels. A 'five-day outlook' summarising fisheries-related environmental conditions, departures from normal and interpretations with respect to fishing operations, is also broadcast twice weekly by high-frequency voice radio. These experimental products are merged with operational products, like 'general weather charts', depicting sensible weather conditions (pressure fields, frontal boundaries, storm tracks, precipitation, wind and wave fields), sea surface temperature measurements, ice analysis, severe storm warnings, like 'five-day outlooks' for general users.

On the basis of the preliminary good results of this programme, it is possible that commercial US users will require in the near future an operational oceanographic satellite system capable of maximising real-time data coverage over the main fishing regions.

Profiting from this application programme limited to the West Pacific Ocean, scientific research should be promoted to investigate the proper method of similar applications for the exploitation and preservation of fish stocks in European waters.

3.6 INLAND USE

Although not specifically designed for land monitoring, an OCM type instrument obviously includes the capability for environmental studies on such applications like vegetation, agrometeorology, hydrology and snow cover. Owing to the low geometric resolution, this applies only to large scale features (>1 km). However, the frequent re-visit time, in comparison to Landsat, permits a multitemporal analysis which can be used in support of high resolution imagery.

The extensive use which is presently being made of the AVHRR data, largely demonstrates the potential interest of this type of applications.

OCM channels 5,8 and 9 (0.64, 1.02 and 1.6 μm) are especially well-suited to describe the vegetation cover of the earth's surface and to analyse the land surface changes in relation with climate as well as to monitor an application such as crop assessment, or to assess the now covered areas, in a better way than with the present wideband AVHRR channels.

3.7 POLLUTION MONITORING

The potential of monitoring pollution in the sea and particularly oil spills by OC techniques has not been fully investigated and thus established yet.

Also the pollution of the air layer above the sea surface, due to organochlorine waste disposal by at-sea

incineration is clearly observable from the colour imagery. More than 100 000 tons of chemicals are yearly incinerated at European and American seas. The monitoring of the released HCl plume, which can spread several hundred kilometers, by conventional methods (ships, airplanes) appears to be insufficient and is connected with many shortcomings.

In coastal areas pollution dispersion is connected with observable phenomena like sediment transport, turbidity and eutrophication.

In conjunction with active and passive microwave techniques, ocean colour however may give useful complementary information.

4. The present situation and the foreseeable future of water colour monitoring from space

In this section the present situation and the foreseeable future in regard to water colour monitoring from space is summarised briefly. (For more details on the systems refer to Annex 2.)

4.1 OCEAN COLOUR MISSIONS

Till now two space missions dedicated to water colour science and applications have been flown, i.e. the Coastal Zone Colour Scanner (CZCS) on the Nimbus-7 satellite and the Ocean Colour Experiment (OCE) of the OSTA-I mission on the second orbital flight test of the Space Shuttle. (Although the Landsat/MSS has been used for the monitoring and mapping of estuarine/coastal turbidity and especially its visual interpretation (50), the instrument is not designed for quantitative analysis of water constituents and large-scale oceanic processes.)

4.1.1 *COASTAL ZONE COLOUR SCANNER AND PROPOSED SYSTEMS*

Since its launch on Nimbus-7 in 1978, the CZCS (see Annex 1, par. 1.1) has produced several scenes which are archived and preprocessed by NOAA and analysed in laboratories of different countries (51). The instrument (design life time: 1 year) will probably be operated till 1984. A steady loss in sensitivity especially in the blue spectral region causes calibration problems which are critical in regard to the atmospheric correction and thus to the interpretation of data.

A modified CZCS was to be included on the National Oceanic System (NOSS) (Annex 1, par. 1.2), which was proposed as an operational demonstration of possible oceanographic data products in near real time. The most important modifications for the CZCS on NOSS (called CZCS II) were the increased number of channels and the increased radiometric resolution. The NOSS programme was deleted at the beginning of 1981. The follow-up programme, the Navy Remote Ocean Sensing System (N-ROSS) presently does not include a multispectral scanner for water colour monitoring.

After the deletion of the NOSS programme and after the removal of the ocean colour monitor from the ERS-1 payload, an attempt was made to consider flying a spare unit of the CZCS on ERS-1. The response was negative (52).

A re-flight of an advanced CZCS, called Ocean Colour Imager (OCI) as part of the operational satellite programmes is studied at present by NASA and NOAA. (Instrument modifications are similar to those for the NOSS/CZCS.) The incorporation of the OCI on the NOAA-J satellite has not been approved yet, however, if this should be the case, a launch could not be expected earlier than around 1989.

4.1.2 *OCEAN COLOUR EXPERIMENT (OCE)*

(see Annex 1, Chapter 2)

One of the six remote-sensing experiments flown during the second flight of the Space Shuttle in November 1981 was the Ocean Colour Experiment (OCE). This consisted basically of a modified aircraft scanner – especially designed for water colour monitoring from high altitude – which was mounted in the cargo bay of the Orbiter and which was operated during the mission above selected portions of the world's oceans. Althoughthe basic objectives of the OCE were met, the OSTA-I mission in general and the OCE data collection in particular were affected to some extent by the frequent delays of the launch date, by the abbreviated mission duration and finally by the prevailing weather conditions, especially along the US coast (52).

In view of the restrictions during the OSTA-I mission, a reflight of the OCE on the OSTA-V mission (early 1986) is presently being discussed.

4.2 PLANNED MISSIONS

4.2.1 *THEMATIC MAPPER (TM) ON LANDSAT-IV*

(Annex 1, Chapter 3)

The restrictions of the Landsat/MSS in terms of water colour monitoring will be compensated to a certain extent by the Thematic Mapper (TM) on Landsat-IV. Improvements of the TM in comparison to the MSS refer to its higher spatial and radiometric resolution, the incorporation of a blue channel and the incorporation of a thermal channel. Monitoring of typical coastal processes will thus be superior, however, the repeat cycle of 16 days (without Landsat D') is considered to be inadequate. The capability of monitoring chlorophyll in open ocean areas depends on the suitability of channel 3 and/or channel 4 to be used for the atmospheric correction of channels 1 and 2. Further, the suitability of the comparatively broad channel 1 (together with channel 2) to determine chlorophyll is still to be proved. The swath width of 185 km is generally too low for the monitoring of large scale oceanic processes. The equator crossing at 9.30 AM limits the area which can still be monitored with suitable sun elevation angles.

4.2.2 *MULTISPECTRAL ELECTRONIC SELF-SCANNING RADIOMETER (MESSR) ON MOS-I*

(Annex 1, Chapter 5)

The Japanese Maritime Observation Satellite I (MOS-I)

is scheduled to be launched in 1987 and includes the MESSR amongst the payload of altogether four instruments. The MESSR is a four-channel multispectral scanner incorporating CCD arrays for monitoring simultaneously two strips of 100 km adjacent to the nadir tracks.

In regard to a quantitative evaluation of water constituents, especially of pigments, the MESSR in its described configuration (54) is most probably unsuitable because a blue channel is not incorporated and the radiometric resolution of 6 bit is too small. Also the swath width is too low for the monitoring of large scale phenomena.

4.2.3 *HIGH-RESOLUTION VISIBLE SENSORS (HRV) ON SPOT*
(Annex 1, Chapter 6)
The payload for the SPOT satellite to be launched after 1984 includes two complementary High-Resolution Visible Sensors (HRV) as shown in Table 13 of Annex 2.

For investigations above water the advantage of this instrument should be seen in applications in which the geometric resolution is of importance rather than those for which a thematic classification of water types is essential. As a result, emphasis will be placed on the monitoring of coastal processes like e.g., the observation of land/water boundaries, tidal flats, estuarine processes, sediment transport and mangrove swamps, rather than of open ocean areas and pigment distribution.

4.2.4 *METRIC CAMERA (M.C.) ON SPACELAB-I*
With a geometric resolution similar to that of the HRV on SPOT, but with a larger FOV and a very high geometric fidelity, the Metric Camera (MC) launched for the first time on the Spacelab Mission I (Nov. 1983) is expected to provide an excellent tool for the monitoring and mapping of land/water boundaries, tidal flats etc. Contrary to these applications, their use for a quantitative mapping of water constituents, like e.g. chlorophyll, will be of less significance.

5. Considerations of an ocean colour mission for ERS-2

5.1 GENERAL

As seen in Chapter 4, in spite of the considerable international interest and support from many scientific and application disciplines, the path-finding CZCS experiment on Nimbus-7 is slowly degrading without a firm plan to replace it by another satellite instrument.

The objectives of this section are to review the definition of an Ocean Colour Monitor (OCM) and the possibility to fly this equipment within the context and constraints of the ESA programme in general and ERS-2 in particular.

5.2 INSTRUMENT TECHNICAL REQUIREMENTS

The technical requirements for an ocean colour monitoring instrument can be derived from the application requirements, identified in section 3 and the need for simultaneous atmospheric observations to correct the ocean colour measurements for atmospheric scattering. With the exception of some fine tuning of the optical channels, the OCWG is of the opinion that the requirements defined for the original OCM were optimised for ocean monitoring. A summary of these requirements is given in Annex 2, together with the principle interface characteristics of the instrument.

This finding of the OCWG does not, however, automatically imply that the original OCM represents the best technical solution to provide for all possible application areas. In particular, it is recognised that the spatial resolution capability of the OCM, which has been seconded to spectral and photometric resolution, may not allow it to fulfill detailed coastal observation requirements. However some of these, such as land/water boundary mapping and small scale turbidity transportation measurements, may be adequately served by other instruments (SPOT HRV or Landsat TM).

5.3 INSTRUMENT TECHNICAL OPTIONS

5.3.1 *THE MECHANICAL SCANNING OCM* (Annex 2)

In order to satisfy all of the technical requirements of the OCM, the original studies clearly determined that an imager utilising a mechanical scanner was preferred. Such an instrument should not be confused with the concept of the thematic mapper of Landsat-D, which is optimised for spatial resolution and represents a technical limit in such developments. In contrast the mechanical scanning OCM has been configured for the requirements of spectral and photometric resolution and to permit the simultaneous co-registration of the large number (13) of spectral bands ranging from 400 to 12 500 nm.

The physical dimensions, and thus to a large extent the development costs, have been maintained at very much more reasonable levels by precisely adopting them to the modest spatial resolution requirements of the global ocean mission. The considerable technological requirements are well-illustrated and have been largely addressed by the RSPP technology programme (see Annex 5).

5.3.2 *STUDIES OF 'ADVANCED' OCM CONCEPTS*

5.3.2.1 *General*

Following requests made by the Remote Sensing Programme Board, the Executive has initiated a total of four studies to investigate alternative technical solutions to measure ocean optical properties. Three of the studies are parallel industrial contracts to investigate 'push-broom' imaging techniques using the so-called CCD technologies; the fourth study, awarded to the University College of London, is aimed at identification of the potential utilisation of imaging photon counting techniques coupled possibly with Fabry-Perot interferometers.

These studies were initiated in November 1982 and have been scheduled for completion in 1983. All of the studies were initiated using the OCM technical constraint of being compatible with the eventual ERS-2.

5.3.2.2 *Preliminary results of the CCD studies*

Following the initial study phase, all three study contractors requested some modifications to the technical requirements at the mid-term review, for basic technological reasons. The major modifications granted by the Agency, in consultation with the OCWG, were:

- reduction of spectral channels to the eight 'visible-near IR' channels;
- reduction of image co-registration requirements from 0.1 to 0.2 pixels;
- reduction of MTF requirements;
- modification of dynamic range requirements.

Each of these changes represent incompatibilities between the original OCM requirements and certain technological limits, essentially:

- lack of suitable IR devices in the foreseen time-scales
- optical design problems to provide ocean coverage in the retained spectral bands
- basic silicon CCD limits
- basic CCD architecture limits.

In contrast, a CCD camera can provide some improvement in spatial resolution, typically 250 m instead of 800 m as specified for the mechanical scanner. This improvement is a natural consequence of the CCD pixel element dimensions and the instrument aperture requirements. (CCD's represent the current optimum detector solution for high spatial resolution.) This implies a higher data rate which may require on-board data reduction to be compatible with a global ocean mission.

5.3.2.3 *Preliminary results of considerations of utilisation of imaging photon counters and Fabry-Perot interferometers*

This study, performed by the University College of London, has been investigating the possibility to fulfill certain aspects of the ocean colour mission utilising the technology developed for certain astronomical and atmospheric scientific objectives. The preliminary results, so far, indicate two possible directions based on the use of:

- imaging photon counters to obtain a push-broom camera configuration to fulfill the visible and near IR channels. It appears feasible to develop a modest cost instrument which would provide a coarse resolution instrument (typically 5 km);
- image photon counters with Fabry-Perot interferometers to generate an imaging Fraunhofer Line Discriminator. The objective of such an instrument is to determine chlorophyll luminescence.

The results of this study will also be analysed by the OCWG.

5.4 CONSIDERATION OF FLIGHT OPPORTUNITIES

An integral part of the ERS-1 phase B activity is the study of the technical requirements to fly an OCM on a second mission (ERS-2). The working assumption for this option is that the OCM could replace the ATSR on the second mission. In order to provide technical guidelines, the Executive has defined an OCM (see Annex 2) which for practical reasons, is a derivative of the original OCM with interface requirements that are as close as possible to the ATSR. The major difference is in the data handling requirements, which impacts the IDHT and, eventually, ground segment requirements. In order to maintain the technological options for an OCM, the studies indicated in section 5.3 have been subject to similar constraints, i.e. the instrument designs will be interchangeable with the ATSR as far as possible.

For reasons of cost to the ERS-1 mission, the subsystem identified as the IDHT, which performs the instrument data handling and transmission, has been optimised for the ERS-1 mission requirements. This will require modification if an OCM mission is to be flown on an ERS-2.

The Executive is also considering the possibilities to fly an OCM mission on other satellites, such as EURECA 2 or ERS-3.

6. Recommendations

6.1 TECHNICAL AND TECHNOLOGY SUPPORT

The ultimate technology requirements for an OCM on ERS-2, or any other satellite, are dependent on the choice of instrumentation. Basically, this choice is between a mechanical scanned instrument and a CCD push-broom scanner. Technology can be broadly identified under the same headings with the exception of some areas in calibration and data distribution and archiving.

6.1.1 *MECHANICAL SCANNING TECHNOLOGY*

The critical areas of this concept were addressed in the RSPP. In general, the work performed remains valid except that the ERS-1 configuration dictates the use of a mechanical cooler similar to the ATSR cooler.

It is the opinion of the working group that it would be inadvisable at present to perform further technological studies for a mechanical scanner unless a definitive commitment is made to fly it. Exceptions can be made in certain areas such as the mechanical cooler where it is essential that the Executive follow-up this type of development.

6.1.2 *PUSH-BROOM TECHNOLOGY*

The studies of both CCD and Imaging Photon Counting techniques have identified the need for significant technology improvements in the areas of optics, spectral separation or filtering, alignment and alignment stability and detector architecture, for example. The specific details are dependent on the actual instrument concept and thus this will require selection before detailing a technology plan.

This comment is not applicable to the more general challenge to develop CCD type technology for the thermal infrared. The OCWG thus *particularly recommends* that the Agency pursues efforts in this area. (Note: it can be expected that a similar recommendation will result from considerations of land application mission requirements where such technology is fundamental to obtaining high spectral resolution imaging in the IR).

6.1.3 *CALIBRATION*

The requirements of calibration are particularly challenging for the OCM mission. These requirements were already partly investigated for the mechanical scanner, but are equally applicable for a push-broom instrument. It should be remembered that an OCM mission requires signal resolution at the level of 5×10^{-4} NE$\Delta\rho$ compared to 5×10^{-3} for a typical land observation instrument such as the HRV or Thematic Mapper.

It can be expected that a push-broom instrument will require significant improvements in data correction areas.

Careful distinction and consideration must be given to all areas of calibration:

- gain calibration (absolute and relative)
- spectral calibration
- on-ground calibration and facilities
- in-flight calibration means and methods both for absolute and relative (detector to detector, channel to channel and instrument with time and temperature) calibration.

6.1.4 *DATA DISTRIBUTION AND ARCHIVING*

The working group has initiated some discussion in this area. A first conclusion is that many data requirements are not real-time requirements because sea structures can have lifetimes of a few days.

As this is an important suggestion which has not been clearly quantified, it forms the basis of a strong recommendation for further work.

The working group will follow-up developments in this area and will further investigate requirements for data acquisition and processing.

6.2 SCIENTIFIC SUPPORT WORK

Previous discussions outline that the complete interpretation of ocean colour measurements from space and its use for applications rely on the following scheme:

1. The correction of atmospheric and sea surface reflection effects to accurately derive the optical properties of the sea water (reflectance, and absorption and scattering coefficients).
2. The relationship between the optical properties of the sea water and its 'bio-physical' properties (e.g. pigment concentration, sediment load, yellow substance, etc.).
3. The use of bio-physical parameters in further models, particularly the use of time series for the study of the dynamics of biological or physical processes (e.g. primary production, upwellings, coastal sediment transport).

Our current scientific knowledge of these mechanisms is sufficient to demonstrate the feasibility and usefulness of the OCM mission. Furthermore, it is possible by now to identify and recommend a number of supporting works related to the OCM mission which should be completed. Their priority can be established with the following criteria:

Priority 1: the information needed by the time of the technical definition of the OCM/ERS-2 (1985) for those having an impact on the technical definition of the experiment.

Priority 2: the information needed before the launch of the satellite (1990) for validation or demonstration experiments.

6.2.1 *PRIORITY 1*

Point 1: Atmospheric and surface reflection correction:
- to obtain the spectral behaviour of sea foam reflectance at wavelengths covered by the OCM (it is suggested that use of Landsat-4/TM experimental data would allow this point to be completed);
- to improve the modelling of the interaction between glitter and atmospheric scattering; and
- to validate the atmospheric correction algorithm (use of Landsat-4/TM data would allow this point to be completed in the range 0.45–2.2 μm with simultaneous ground/sea truth measurements).

Point 2: Optical properties versus bio-physical properties of sea water:
- to acquire high spectral resolution measurements in order to improve the relationship between the optical properties (reflectance, absorption and scattering coefficients, fluorescence efficiency) and the bio-physical parameters in order to make a final tune of the OCM spectral bandpass in 1985 (this may be done mainly from ship-borne/air-borne measurements;
- to further analyse the spectral bandwidth requirements, and particularly the impact of the spectral bandwidth on the accuracy of the retrieval of the bio-physical parameters.

6.2.2 *PRIORITY 2*

- to demonstrate the feasibility (validation of algorithms) and usefulness of the OCM for potential applications with aircraft or Shuttle experiments;
- to encourage further use of bio-physical parameters in dynamic models (e.g. biology: phytoplankton and primary production, or oceanography: sediment transport and surface circulation modelling) with the aid of present time series of CZCS data.

7. Illustrated demonstrations of ocean colour use in science and services

Although the availability of the CZCS data from Nimbus-7 has not been extensive to European investigators for a variety of reasons, a few images, processed in different countries, of the European waters (eastern Atlantic, the Channel, and the Mediterranean Sea), demonstrate the potentials of ocean colour for a variety of applications in science and in public services.

The extensive scientific studies of the available data have permitted a substantial improvement in ocean colour sensing techniques for the next generation of sensors. The OCM compared to the CZCS as shown in Annex 3 is a demonstration of the possible improvement in quality of the colour sensing and of the considerable improvement in the correction of signals for atmospheric effect (aerosol).

A few examples of colour images from the CZCS are here presented to demonstrate, at the present stage, how the ocean colour has been of great help in several scientific domains starting from the exploration and discoveries of features which were never described by conventional oceanographic methods nor models. They have opened a new interest in the sea surface and lower atmosphere interaction and in coastal processes which are connected to a variety of phenomena and of calamities for human properties.

No exercise has been made yet, of the direct use of ocean colour for fisheries in European waters because a great deal of research is still needed and because the information has not been so far sufficiently frequent. Examples are shown, however, of applications in the eastern Pacific (California area) which have been more than experimental (Figs. 8, 9).

The following series of Figures 1 to 7 deal with European waters and are representative of various applications and uses of the colour imagery. Some brief explanations are given about the methods used to process the data and each figure is provided with a comment (caption) about the problem addressed and the main features observed from space.

The CZCS scenes (Figures 1,2,3,4 and front cover) have been processed by A. Bricaud & A. Morel (Laboratoire de Physique & Chimie Marines, Villefranche) according to a method which derives from that developed by the Nimbus Experiment Team (NET – Report SASC No.EAC-T-8085-0027) and in use at NASA.

With respect to this 'standard' pixel-by-pixel method, several modifications have been introduced: the 'noarmised water-leaving radiance' concept, originally developed by Gordon & Clark (38) in order to estimate the Ångström exponent for the aerosol scattering, has been generalised (40) for two purposes:

- to allow the estimate of the aerosol spectral effect to be effected even in case of moderately productive waters (not only in case of 'clear waters' as in Gordon's method);
- to provide a tool for discriminating between Case 1 waters and sediment-dominated waters.

These improvements rest on a modelling of the ocean reflectance in relation to biogenous material content, developed for Case 1 waters only (39). They are associated with iterative computations which are performed for each pixel and each channel. The computation time is multiplied by a factor between 2 and 5 with respect to the standard method. Finally, as soon as Case 1 waters are indubitably identified (owing to the computation of normalised water-leaving radiances), the algorithm combining the corrected radiances which is used for the pigment retrieval is:

$$(mg/m^3)\, C = 1.73\,(L_{443}/L_{550})^{-2.04}$$

This algorithm is close to that presented before (ref. 5, and Table 1 in Annex 4), except it has been adjusted for the actual CZCS bands. For high pigment concentrations ($C = 1.5\ mg/m^3$), the algorithm which is used is:

$$(mg/m^3)\, C = 2.51\,(L_{520}/L_{550})^{-6.38}$$

The Case 2 waters, for which the above algorithms fail (or are uncertain), are excluded (black mask). Conversely, a black mask is put on Case 1 waters (ex. Figure 2a), and the values of the normalised water-leaving radiance in channel 3 (550 nm) are then visualised (increasing values from light yellow to dark red) in the area of the scene where Case 2 waters are present. These 'normalised' radiances, by definition, are independent of the viewing and lighting conditions (they are computed as if the sun was at zenith for all pixels and as if the atmosphere was not absorbing). Thus these normalised radiances are meaningfully comparable and depict the turbidity (sediment load) at least in a qualitative way; a quantitative estimate would imply a local study of the relationships between the sediment load and the reflectance (to which the normalised radiance is proportional, through a geometrical factor).

For Figures 1 to 4 (dealing with Case 1 or Case 2 waters), clouds *and* land are displayed in white. The thermal images (channel 6) are uncorrected and not provided

with absolute temperatures; the relative temperature increases from dark, medium blue, then green, yellow, orange and finally red (6 steps).

The CZCS scenes of the western English Channel (Figs. 5 & 6) have been processed by P.M. Holligan & al.

Blooms of the dinoflagellate, *Gyrodinium aureolum*, are reported each year from areas where fronts form in response to tidal mixing or upwelling. These include the Hattegat and south coast of Norway, Helgoland, northwest North Sea, Irish Sea, southwest Ireland and the western English Channel. The standing crops of chlorophyll *a* and phytoplankton carbon can exceed 500 mg/m^2 and 50 g/m^2 respectively, giving a chocolate-brown colour to the water and extinction coefficients at 550 nm as high as 0.5/m. In coastal regions extensive mortalities of fish and benthic animals have been associated with the blooms.

In 1981, *G. aureolum* was abundant in the surface waters of the western English Channel from early July to the end of August. Due to very weak backscattering by the plant cells (up to 8000/ml), the extent of the bloom was not apparent on single channel CZCS images (Fig. 5a) even after correction for atmospheric effects. However, a chlorophyll algorithm based on the ratio of reflectances for channels 2 (520 nm) and 3 (550 nm) (Fig. 5b) gave an overall accuracy for total chlorophyll, C (chlorophyll + phaeopigment) of log C $\pm$0.26 when compared to field measurements (Fig. 5c). By the end of July the extent of the bloom was 30 000 km^2 (Fig. 5b) and corresponded to a region of anomalously warm surface water to the stratified side of the tidal front (Fig. 5d). The maximum chlorophyll *a* levels at this time were 70 mg/m^3.

Since 1979 CZCS images have shown the regular occurrence of patches of 'high reflectance water' along the shelf edge between 45°N and 60°N during the spring and early summer. This phenomenon is caused by coccolithophores, phytoplankton with external plates or coccoliths of calcium carbonate which give rise to 'white water' conditions due to strong backscattering of visible light. In shelf waters, the widespread oceanic and neritic species, *Emiliania huxleyi*, is generally dominant.

In 1982 a coccolithophore population in the Celtic Sea was apparent on CZCS images (Channels 1-3) between mid-May and early June (Fig. 6). Observations at sea at the end of May showed 1–2 mg/m^3 chlorophyll *a* in the coccolithophore water, compared to values up to 2.5 mg/m^3 for areas where diatoms and dinoflagellates were dominant. Under these conditions the normal channel ratio or difference algorithms for chlorophyll are not reliable. However, a significant correlation was found between the reflectance of visible light and the surface abundance of coccolithophores. The maximum densities of cells and detached coccoliths were 10^4 and 10^5/ml respectively, giving up to 40 g/m^2 calcite. This material is thought to be the major form in which biogenic carbon is being deposited, mainly on the continental slope.

The CZCS scene (Fig. 7) of the north Adriatic Sea was processed by V. Barale of the Istituto Studio Dinamica Grandi Masse in Venice. The diffuse attenuation coefficient (76) was computed with the algorithm developed at Scripps (Austin & Perzold, see Annex 4, Table 1). Other algorithms are being developed for this area of very complex turbid Case 2 waters.

The diffuse attenuation coefficient has been of help in representing the distribution and dynamics of the polluted and relatively cold Italian coastal waters of the Adriatic where runoff from six rivers and of the Lagoon of Venice are mixed. Cloud free visible and IR images in different seasons, through 1979–80, were correlated with mathematical models of circulation. IR images are at times complementary and at other times not correlated to the surface water turbidity. Figure 7c in fact shows an apparent cool skin water which is probably due to atmospheric haze covering the sea surface.

The false colour image (Fig. 7b) shows a cyclonic eddie in the north Adriatic which recurs often and which very probably contributes to the development of eutrophism, a calamity which has been ever more frequent during the last few years, with the death of thousands of tons of fish and great damages to the Italian amenities of sandy beaches from Venice to Ravenna.

Figure 1a
Western Mediterranean, South of Sardinia; 22 March 1979 (orbit 2062). The pigment concentrations range from lesser than 0.06 (deep blue) to greater than 0.12 mg/m³ (dark green). The pigment concentrations evidence a 150 km elliptical gyre, which was recorded also on the images of 24 March (see cover) and 13 April (not shown here). The corresponding thermal imagery exhibits at the location of the gyre a warmer spot without any filament-like structures, even with a 0.2° resolution (one digital count).

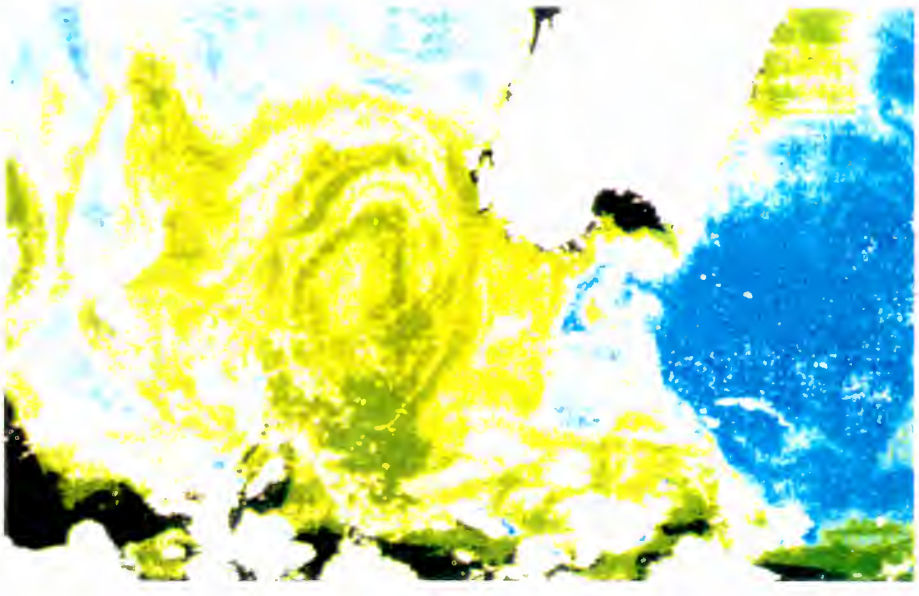

Figure 1b
In the same area, near Sardinia; 5 June 1981 (orbit 13200). The range of pigment concentration goes from lesser than 0.25 (blue) to greater than 0.40 mg/m³ (green). (The brown patches represent turbid Case 2 waters). The big dynamical structure (about 120 km) originates from meanders of Atlantic waters along the Algerian coast. These waters are depicted by their higher pigment concentrations. The anticyclonic eddy with its smaller cyclonic companion exhibits no signature in the simultaneously acquired thermal image of the skin temperature.

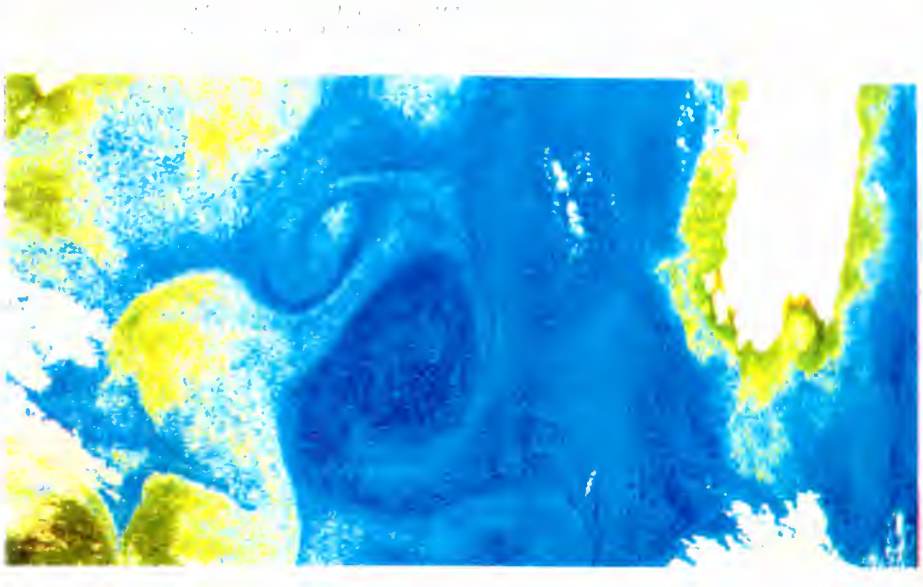

Both these images exemplify how the phytoplanktonic pigment concentration can be assessed from space with a high sensitivity and how the spatial-temporal evolution of the algal biomass can be described over vast zones. They also demonstrate that dynamical structures can be revealed through the bio-optical properties of the surface layer.

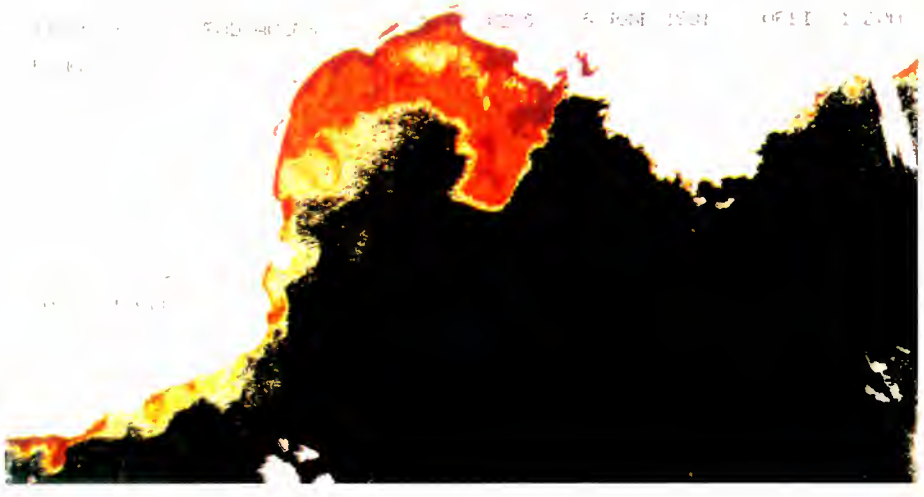

Figure 2a
Gulf of Lions, 5 June 1981 (orbit 13200). The image is processed for Case 2 waters masking Case 1 waters (black). The normalised water radiances, at 550 nm (increasing from yellow to dark red with increasing turbidity), indicate the sediment load. The snow melting has increased the runoff of the Rhône River. The sediments, from the delta, have invaded the major part of the Gulf and join the turbidity in the shallow waters along the sandy coast of Languedoc.

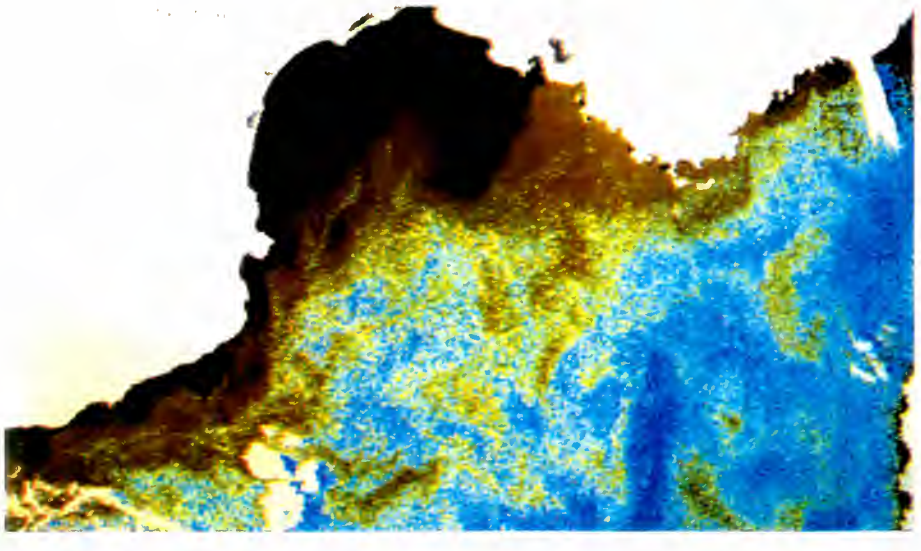

Figure 2b
The same image processed for case 1 waters masking the turbid case 2 waters (black). The pigment concentrations decrease from offshore (lesser than 0.25 mg/m^3, dark blue) to nearshore around the turbid zone (0.60 mg/m^3, brown). The nutrient enrichment due to the fresh water outflow induces an enhanced primary production.

By repeated images through the years, coastal processes and primary production variations can be represented very effectively for planning management and control.

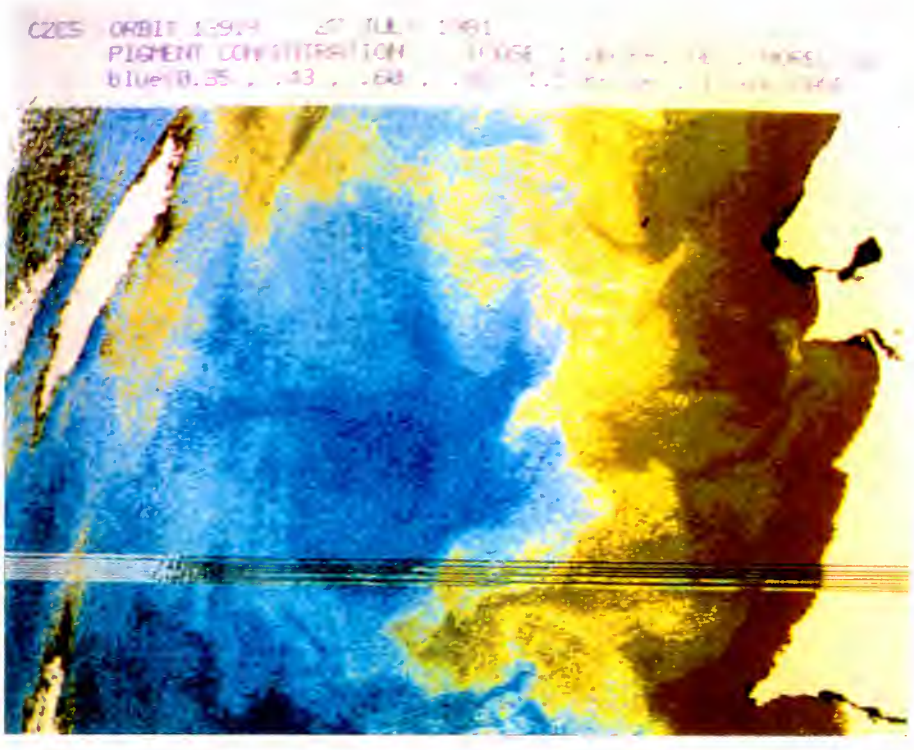

Figure 3a
Atlantic Ocean, West of Portugal; 27 July 1981 (orbit 13919). Pigment concentration, from lesser than 0.35 to higher than 1.5 mg/m³ (from blue to brown), is distributed along the coast within an approximately 100 km wide band. This high phytoplankton development is linked to the coastal upwelling generated by the trade winds, blowing at this season.

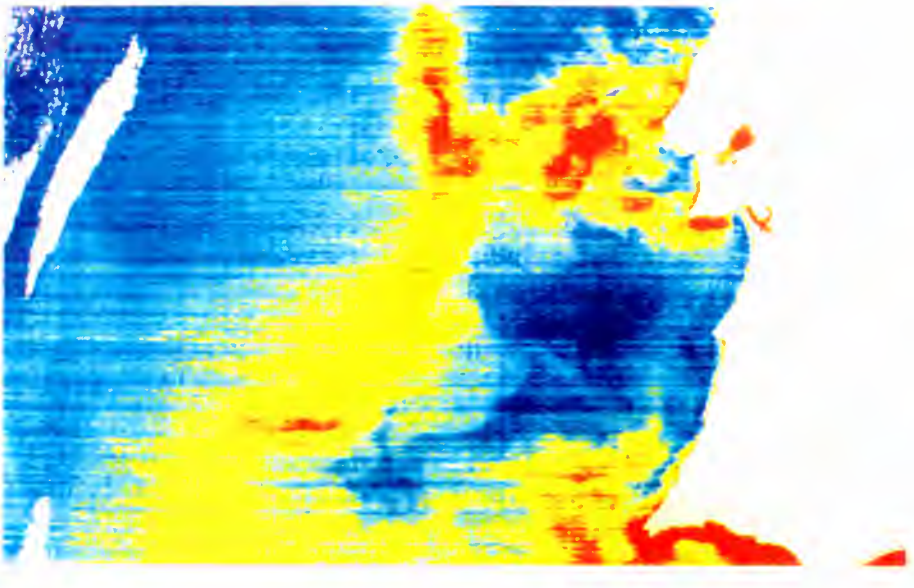

Figure 3b
Thermal imagery, from red (warm) to blue (cold) in 0.40°C steps, shows the upwelled cold waters drifting from the coast toward SW and a warmer zone off Lisbon. The thermal and visible imageries appear non-redundant, with complementary informations.

By the combined simultaneous IR and visible images, the ocean mechanisms, both dynamical and biological, their interaction and their variations can be more accurately explained.

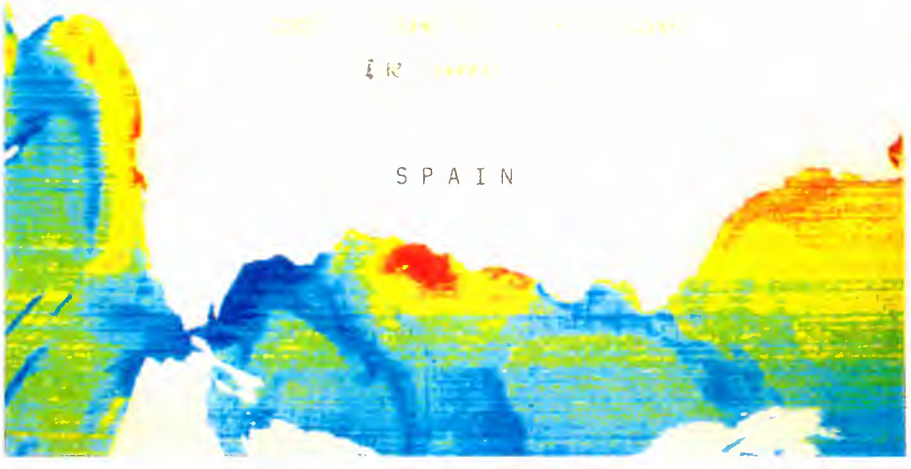

Figure 4a
Gibraltar Strait and Alboran Sea; 5 June 1981 (orbit 13200). The thermal imagery, is processed in six colours from blue (cold) to red (warm) with a 0.72°C step between each colour. The cold Atlantic waters enter the Alboran Sea deflecting north and then into an anticyclonic gyre followed by a meander further East. The cold upwelled waters, (along the Spanish coast, East of Gibraltar) associated with the Atlantic 'jet' are strongly marked.

Figure 4b
The pigment concentration from deep blue to dark green in six steps (0.5, 0.8, 1.3, 1.8, 2.5 mg/m^3) indicates that the phytoplankton-rich waters are associated with the Atlantic inflow and the coastal Spanish upwelling. Surrounded by the Atlantic current, several cores of Mediterranean surface waters are identified by their lower algal content.

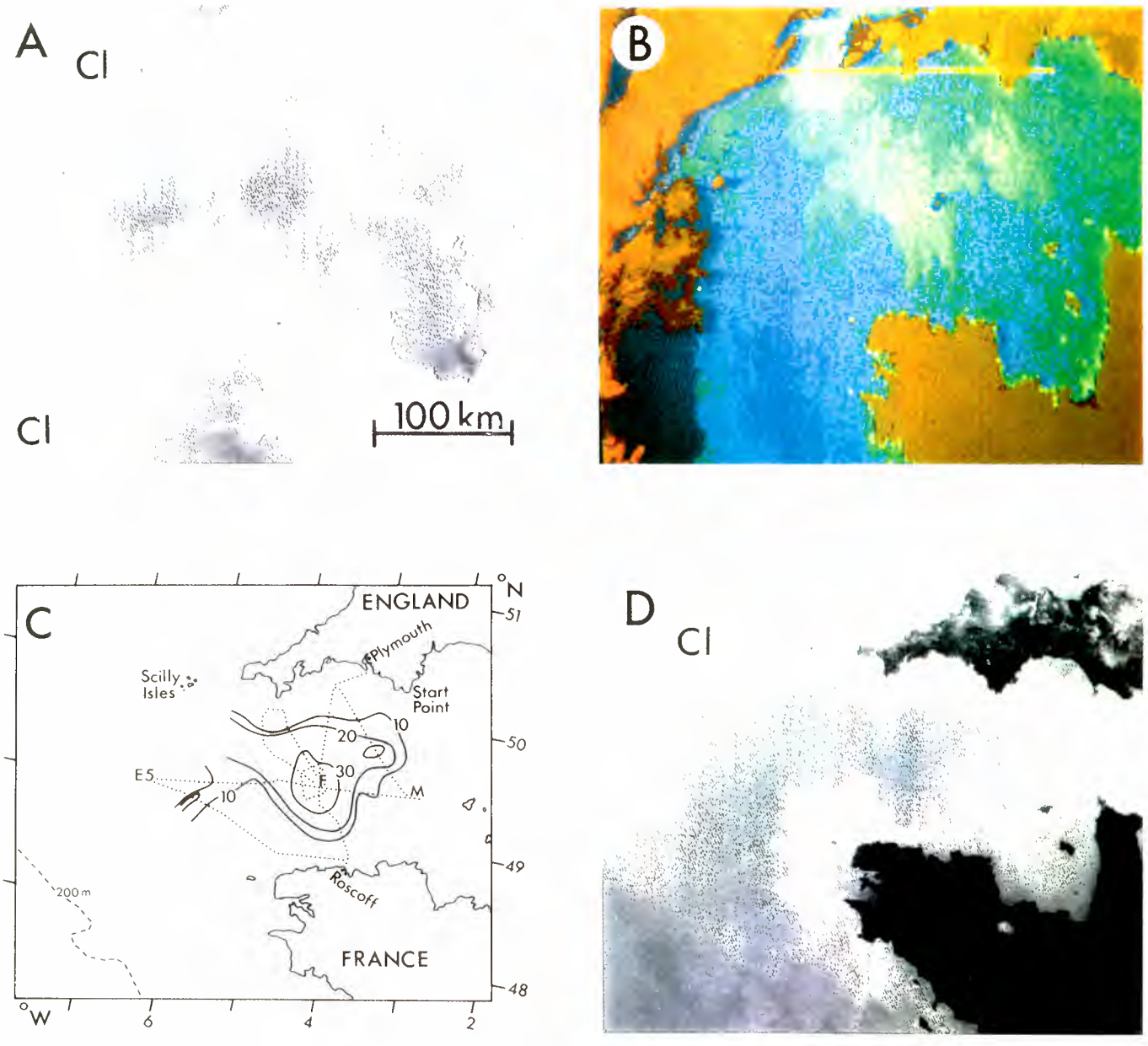

Figures 5. (a) Uncorrected CZCS channel 3 image of the western English Channel for 29 July 1981 (Cl = clouds).
(b) Corresponding image of surface chlorophyll distribution, based on the ratio of channels 2 to 3, for July 29 1981. Land appears brown and clouds red.
(c) Surface chlorophyll a (mg/m³) distribution derived from ship observations, 23 July–2 August 1981. The dotted line indicates the ship's track.
(d) NOAA-6 infrared surface temperature image for 29 July 1981. The dark areas are relatively warm. Note that the geometric distortion is less severe than on the CZCS images (a,b).

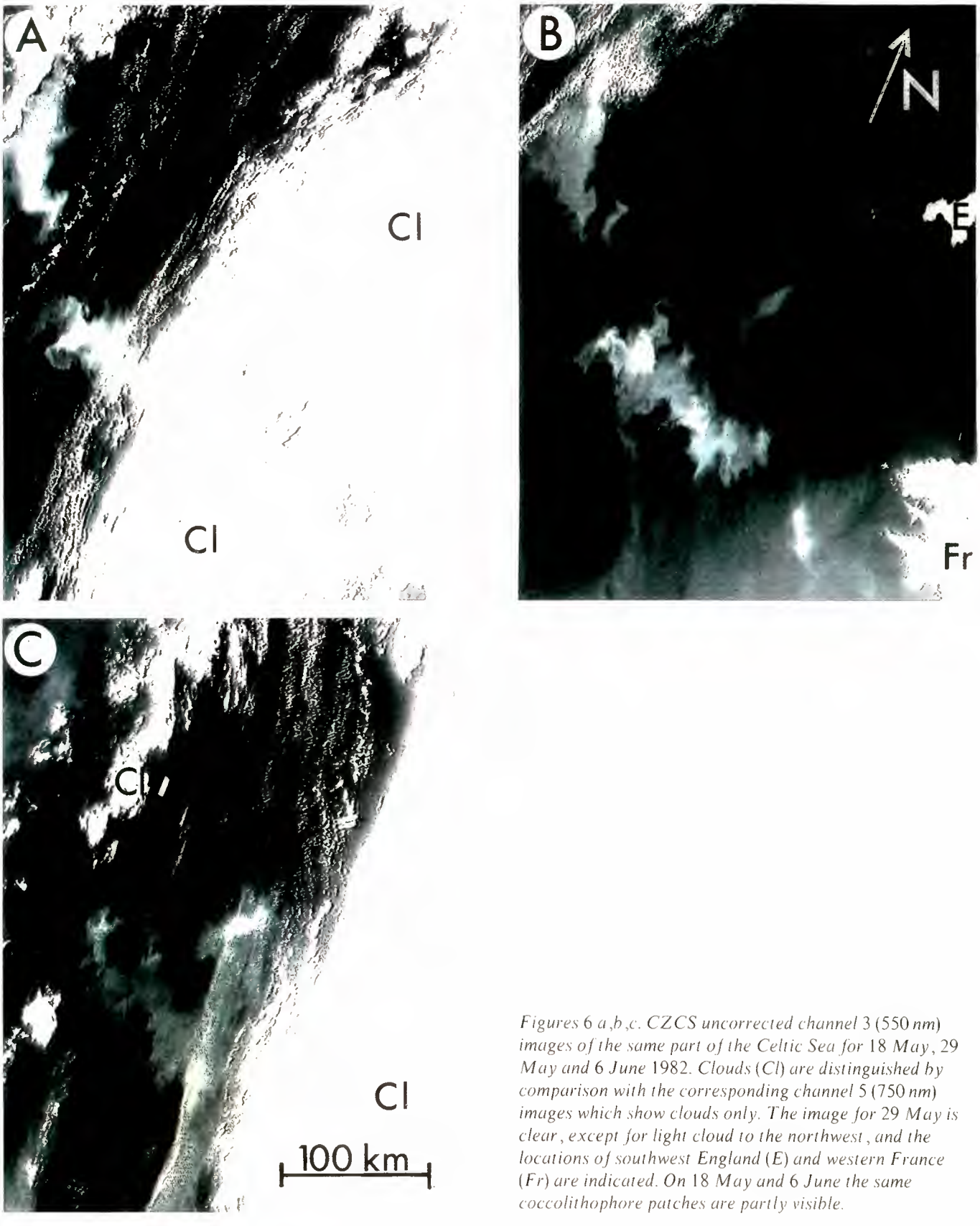

Figures 6 a,b,c. CZCS uncorrected channel 3 (550 nm) images of the same part of the Celtic Sea for 18 May, 29 May and 6 June 1982. Clouds (Cl) are distinguished by comparison with the corresponding channel 5 (750 nm) images which show clouds only. The image for 29 May is clear, except for light cloud to the northwest, and the locations of southwest England (E) and western France (Fr) are indicated. On 18 May and 6 June the same coccolithophore patches are partly visible.

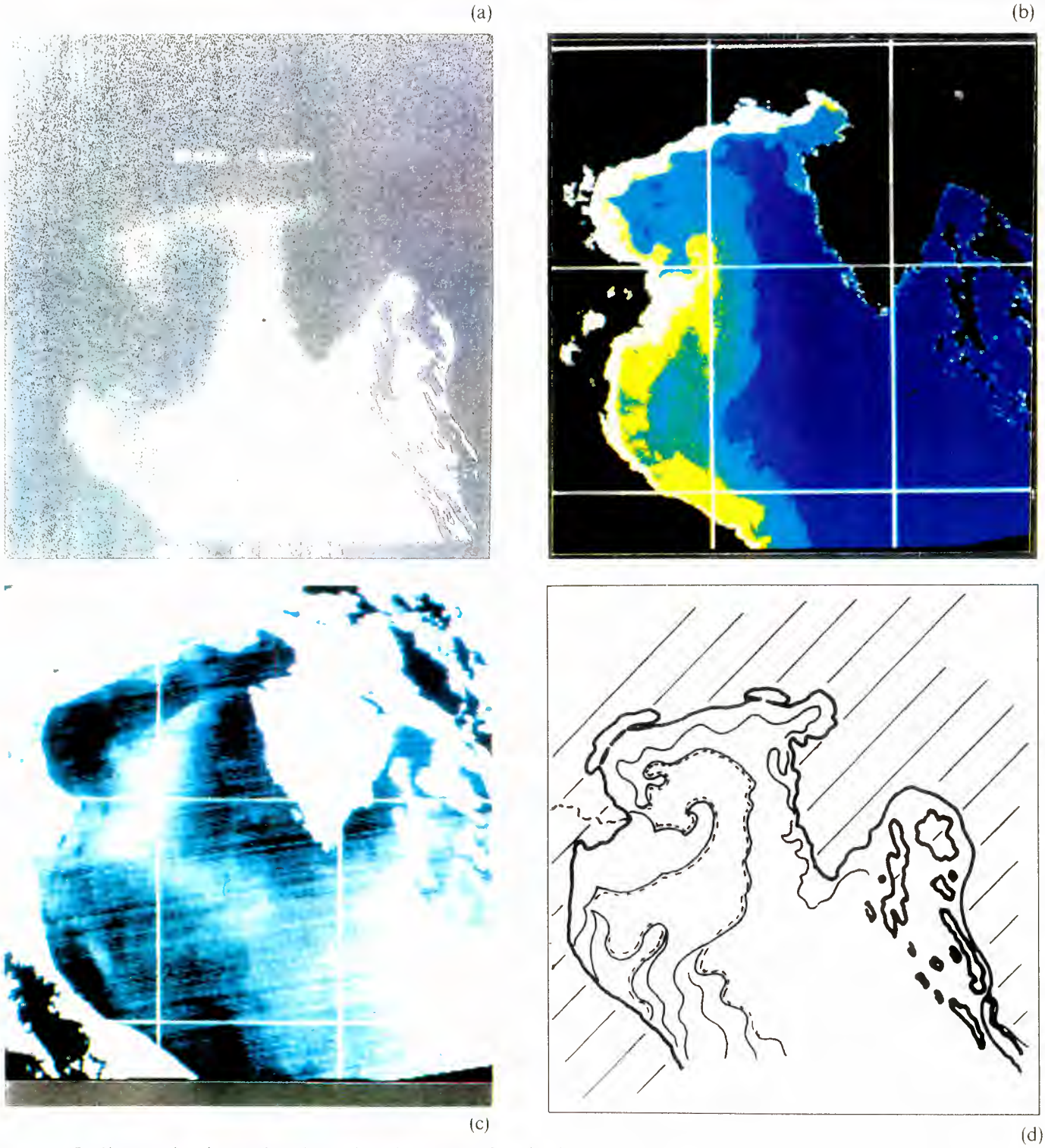

Figure 7. The North Adriatic Sea; 3 April 1979 (orbit 2228). The first figure (7a) shows the distribution of the 'blue to green' ratio which is likely for this zone less informative than the diffuse attenuation coefficient (7b; the colour encoding corresponds to arbitrary degree of concentration); the main features, particularly the cyclonic eddy, as schematically drawn in 7d, do not exhibit a corresponding thermal signature (7c).

By repeated images from 15 December 1978 to 29 July 1979 the seasonal variations of surface water masses of the Adriatic Sea have been represented for the first time.

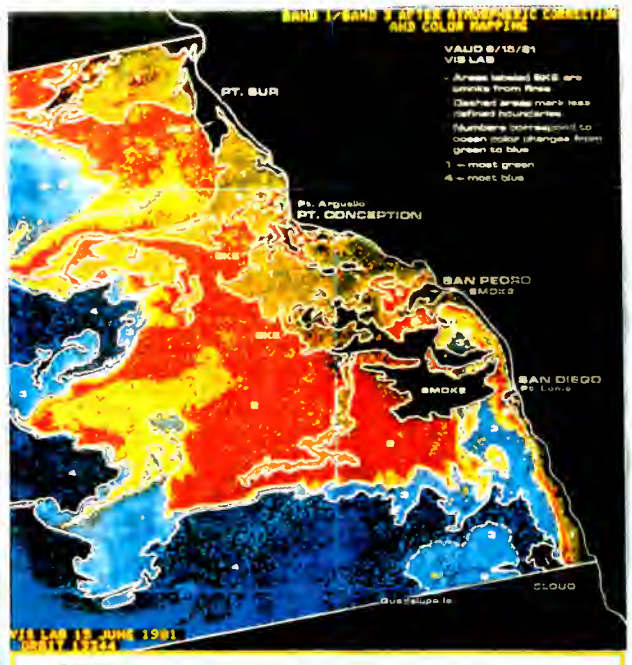

CZCS image of the ocean surface (shown above) using false color to highlight key color regions & boundaries.

Scientific and commercial studies of Seasat data, along with investigations of a Coastal Zone Color Scanner (CZCS) currently in orbit on the Nimbus-7 satellite, have identified promising techniques that may be used to improve the analyses and forecasts of ocean-surface features.

It now has been demonstrated conclusively that wave heights, sea-surface directional wind velocities, sea-surface temperature, and topography can be measured from space. This information can be used in such economic and social applications as improving the efficiencies of weather or sea-state-related operations in the marine industries; providing better warning of severe wind, rain or wave conditions; providing a means of improving and managing the resource yield in many marine industries; providing improved navigation through ice and currents; and creating a better understanding of the ocean and its dynamics.

Nimbus-7 Coastal Zone Color Scanner (CZCS) image of ocean surface before processing for color boundaries

Nimbus-7 CZCS image processed to show color boundaries and possible chlorophyll concentrations.

NASA
National Aeronautics and Space Administration

Figure 8. CZCS images and colour mappings for ocean dynamics (NASA).

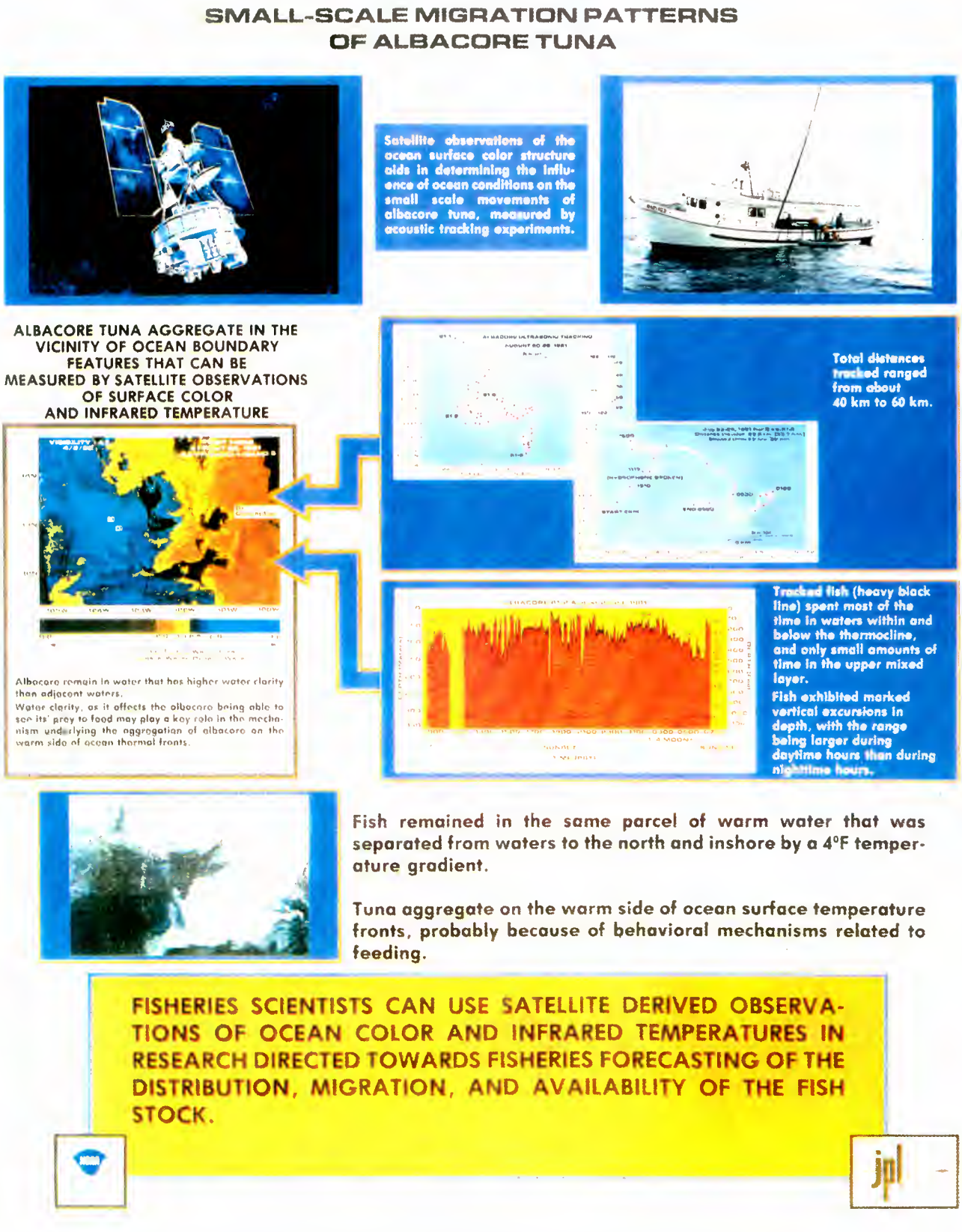

Figure 9. CZCS images Fishery forecasting in the Pacific.

8. References and bibliography

1. Preisendorfer, R W, 1961. Application of radiative transfer theory to light measurements in the sea, *UGGI Monogr. No.* 10 (Symposium on Radiant Energy in the Sea), 11 – 30.
2. Gordon, H R, O B Brown & M M Jacobs, 1975. Computed relationships between the inherent and apparent optical properties of a flat homogeneous ocean, *Applied Optics*, 14, 417 – 427.
3. Prieur, L & A Morel, 1975. Relations théoriques entre le facteur de réflexion diffuse de l'eau de mer à diverses profondeurs et les caractéristiques optiques (absorption, diffusion), *IAPSO-IGGU XVI General Assembly* (Grenoble).
4. Kirk, J T O, 1981. Monte Carlo study of the nature of the underwater light field in, and relationships between optical properties of, turbid yellow waters, *Aust. J. Mar. Freshwater Res.*, 32, 517 – 532.
5. Morel, A, 1980. In-water and remote measurement of ocean colour, *Bound. Layer Meteor.*, 18, 177 – 201.
6. Bricaud, A, A Morel & L Prieur, 1981. Absorption of dissolved organic matter of the sea ('yellow substance') in the UV and visible domains, *Limnology and Oceanography*, 26, 43 – 53.
7. Baker, K S & R C Smith, 1982. Bio-optical classification and model of natural waters, *Limnology and Oceanography*, 27, 3, 500 – 509.
8. Morel, A & A Bricaud, 1981 a. Theoretical results concerning the optics of phytoplankton, with special reference to remote sensing applications, In: 'Oceanography from Space', (ed.) J F R Gower, *Mar. Sci.*, Plenum Press (NY), Vol. 13, 313 – 328.
9. Morel, A & A Bricaud, 1981 b. Theoretical results concerning light absorption in a discrete medium and application to the specific absorption of phytoplankton, *Deep Sea Res.*, 28A, 11, 1357 – 1393.
10. Gordon, H R & D K Clark, 1980 b. Atmospheric effects in the remote sensing of phytoplankton pigments, *Boundary Layer Meteorology*, 18, 299 – 313.
11. Smith, R C & W H Wilson, 1981. Ship and satellite bio-optical research in the California Bight, In: 'Oceanography from Space', (ed.) J F R Gower, Plenum Press (NY), *Marine Science*, Vol. 13, 281 – 294.
12. Austin, R W & T J Petzold, 1981. The determination of the diffuse attenuation coefficient of sea water using the coastal zone colour scanner, In: 'Oceanography from Space', (ed.) J F R Gower, Plenum Press (NY), *Mar. Sci.*, Vol. 13, 239 – 256.
13. Clark, D K, 1981. Phytoplankton algorithms for the Nimbus-7 CZCS, In: 'Oceanography from Space', (ed.) J F R Gower, Plenum Press (NY), *Mar. Sci.*, Vol. 13, 227 – 238.
14. Gordon, H R & W R Cluney, 1975. Estimation of the depth of sunlight penetration in the sea for remote sensing, *Appl. Optics*, 14, 413 – 416.
15. Gordon, H R & D K Clark, 1980. Remote sensing optical properties of a stratified ocean: an improved interpretation, *Appl. Optics*, 19, 3428 –
16. Morel, A, 1982. Optical properties of radiant energy in the waters of the Guinea dome and the Mauritanian upwelling area in relation to primary production, Rapp. P-v. Reun. Cons. Int. Explor. Mer., 180, 87 – 100.
17. Gordon, H R & A Y Morel, 1983. Remote assessment of ocean colour for interpretation of satellite visible imagery: a review, Lecture notes in Coastal & Estuarine Studies series, Springer-Verlag, NY (4, pp. 114).
18. Woodwell, G M, R H Whittaker, W A Reiners, G E Likens, C C Delwiche & D B Botkins, 1978. The biota and the world carbon budget, *Science*, 199, 141 – 146.
19. Walsh, J J, G T Rowe, R L Iverson & C P Mcroy, 1981. Biological export of shelf carbon is a neglected sink of the global CO_2 cycle, *Nature*, 291, 196 – 201.
20. Eppley, R W, 1980. Estimating phytoplankton growth rates in the central oligotrophic oceans. Primary productivity in the sea, *Envir. Sci. Res.*, 19, (ed.) P G Falkowski, Plenum Press (NY), Vol. 19, 231 – 242.
21. Gieskes, W W C, G W Kraay & M A Baars, 1979. Current ^{14}C methods for measuring primary production: gross under-estimates in oceanic waters, *Neth. J. Sea Res.*, 13, 58 – 78.
22. Smith, R C & K S Baker, 1981. Oceanic chlorophyll concentrations as determined using Coastal Zone Colour Scanner imagery, *J. Mar. Biol.*, 66, 269 – 279.
23. Smith, R C, R W Eppley & K S Baker, 1982. Application of satellite CZCS chlorophyll images for the study of primary production in southern California coastal waters, *J. M. Mar. Biol.*, 66, 281 – 288.
24. Gauthier, C, 1982. Mesoscale insolation variability derived from satellite data, *J. of Appl. Met.*, 21, 1, 51 – 58.
25. Morel, A, L Prieur & S Sathyendranath, 1983. Rapport final contrat ESA 4726-81 F.
26. Morel, A & L Prieur, 1977. Analysis of variations in ocean colour, *Limnology and Oceanography*, 22, 709 – 722.
27. Neville, R A & J F R Gower, 1977. Passive remote sensing of phytoplankton via chlorophyll fluorescence, *J. Geophys. Res.*, 82, 24, 3487 – 3493.
28. Gordon, H R, 1979. Diffuse reflectance of the ocean: the theory of its augmentation by chlorophyll fluorescence at 685 nm, *Appl. Optics*, 18, 8, 1161 – 1166.
29. Loftus, M E & H H Seliger, 1975. Some limitations of the in vivo fluorescence technique, *Chesapeake*

Sci., 16, 2, 79 – 92.

30. Whitlock, C W, L R Poole, J W Usry, W M Houghton, W G Witte, W D Morris & E A Gurganus, 1981. Comparison of reflectance with backscatter and absorption parameters for turbid waters, *Appl. Opt.*, 20, 3, 517 – 522.
31. Spitzer, D & al., 1982. Preprint Volume: 'First International Conference on Meteorology and Air/Sea Interaction of the Coastal Zone', May, The Hague, 296.
32. Bukata, R P, J E Bruton, J H Jerome, S C Jain & H H Zwick, 1981. Optical water quality model of Lake Ontario, 2. Determination of chlorophyll *a* and suspended mineral concentrations of natural waters from submersible and low altitude optical sensors, *Appl. Opt.*, 20, 9, 1704 – 1714.
33. Witte, W G, C J Whitlock, R C Harris, J W Usry, L R Poole, W M Houghton, W D Morris & E A Gurganus, 1982. Influence of dissolved materials on turbid waters. Optical properties and remote sensing of reflectance, *J. Geophys. Res.*, 87 – 441.
34. Gower, J F R and G Borstad, 1981. Use of the in vivo fluorescence line at 685 nm for remote sensing surveys of surface, In: 'Oceanography from Space', *Marine Sci.* (ed.) J F R Gower, Plenum Press (NY), Vol. 13, 329 – 346.
35. Mueller, J L & P E La Violette, 1981. Colour and temperature signatures of ocean fronts observed with the Nimbus 7 CZCS, In: 'Oceanography from Space', *Mar. Sci.*, (ed.) J F R Gower, Plenum Press (NY), Vol. 13, 295 – 302.
36. Sathyendranath, S & A Morel, 1983. Light emerging from the sea: interpretation and uses in remote sensing, In: '*Remote Sensing Applications in Marine Science and Technology*', A P Cracknell (ed.), D. Reidel Publ. Co., Ch. 16, 323 – 357.
37. Gordon, H R & D K Clark, 1981. Clear water radiances for atmospheric correction of CZCS imagery, *Appl. Opt.*, 20, 4175 – 4183.
38. Gordon, H R, D K Clark, J W Brown, O B Brown, R H Evans & W W Broenkow, 1983. Phytoplankton pigment concentrations in the Middle Atlantic Bright: comparisons of ship determinations and CZCS estimates. *Appl. Opt.*, 22, 20 – 36.
39. Morel, A, 1983. Optical modelling of the upper ocean attenuance and reflectance in relation to biogenous material content ('Case 1' waters), *IUGG/IAPSO Hamburg*, Abstract, Vol. PS7, 148 – 149.
40. Bricaud, A & A Morel, 1983. Interferences between atmospheric corrections and in-water algorithms in CZCS imagery processing: a re-examination of the problem, *IUGG/IAPSO*, *Hamburg*, Abstract, Vol. PS7, 150.
41. Sturm, B. & Tassan, 1983. An algorithm for sediment retrieval from CZCS data with low sensitivity to the atmospheric correction uncertainties (to be published).
42. Bethoux, J P & L Prieur, 1983. Hydrologie et circulation en Méditerranée nord-occidentale, *Pétroles & Techniques*, 299, 25 – 34.
43. Prieur, L & S Sathyendranath, 1981. An optical classification of coastal and oceanic waters based on the specific spectral absorption curves of phytoplankton pigments, dissolved organic matter and other particulate materials, *Limnology and Oceanography*, 26 (4), 671 – 689.
44. Bricaud, A, A Morel & L Prieur, 1983. Optical efficiency factors of some phytoplankters, *Limnology & Oceanography*, 28 (5), 816 – 832.
45. Platt, T & al., 1977. Modelling productivity of phytoplankton, *The Sea*, Wiley Interscience (NY), 6, 807 – 856.
46. Walsh, J J, 1980, Marine photosynthesis and the global carbon cycle, 'Primary Productivity in the Sea', P G Falkowski (ed.), Plenum Press (NY), 497 – 506.
47. Woods, J D, W Barkman & A Horch, 1983. Solar heating of the world, submitted to *Ocean Quart. J. Roy. Meteor. Soc.*
48. Woods, J D, 1983. Satellite monitoring of the ocean for global climate research, *Phil. Trans. R. Soc.*, London.
49. Arnone, R A & B E Arthur, Jr., Interpretation of hydrographic features using Landsat images, NORDA Report 39.
50. NASA, Goddard Space Flight Center, 1978. *The Nimbus-7 User's Guide*, August, C R Madrid (ed.).
51. ESA 'Investigations of technical feasibility to embark the Coastal Zone Colour Scanner on ERS-I, ESA/PB-RS (82), 5.
52. Kim, H H & W D Hart, 1982. The results of an initial analysis of OSTA-I/Ocean Colour Experiment (OCE) imagery, NASA, TM 83943 (May).
53. Ishizawa, Y, R Kuramasu & R Nagura, 1980. Multispectral Electronic Self-Scanning Radiometer for MOS-I, *XXXI Congress of the Intern. Astron. Federation*, *Tokyo*.
54. NASA, Goddard Space Flight Center, 1982. *MAREX*, Report of the Ocean Color Science Working Group, December.

Annex 1

Detailed Description of Sensors applied to Water Colour Monitoring from Space

As pointed out in Chapter 4 of this report, a more detailed analysis of the ocean colour sensors mentioned there is added here for the interested reader. It should also help to compare typical instrument/platform features. In view of the uncertainties regarding future programmes, emphasis is placed on those monitoring systems which have been operated during the past or which are still operating at present.

1. Coastal Zone Color Scanner (CZCS)

1.1 *NIMBUS-7/CZCS*

Nimbus-7 is the latest satellite in a programme initiated by NASA in the early 1960's and carries a highly advanced payload of 8 different meteorological, oceanographic and earth surface sensing instruments (Fig. 1). The orbital parameters for the satellite are listed in Table 1.

Table 1. *Nimbus-7 orbit specifications.*

Altitude	955 km
Node	ascending
Re-visit time	6 days
Orbit	sunsynchronous
Separation	26°
Inclination	99.2°
Equator crossing	noon
Orbit time	104 mn
Orbits/day	13.8

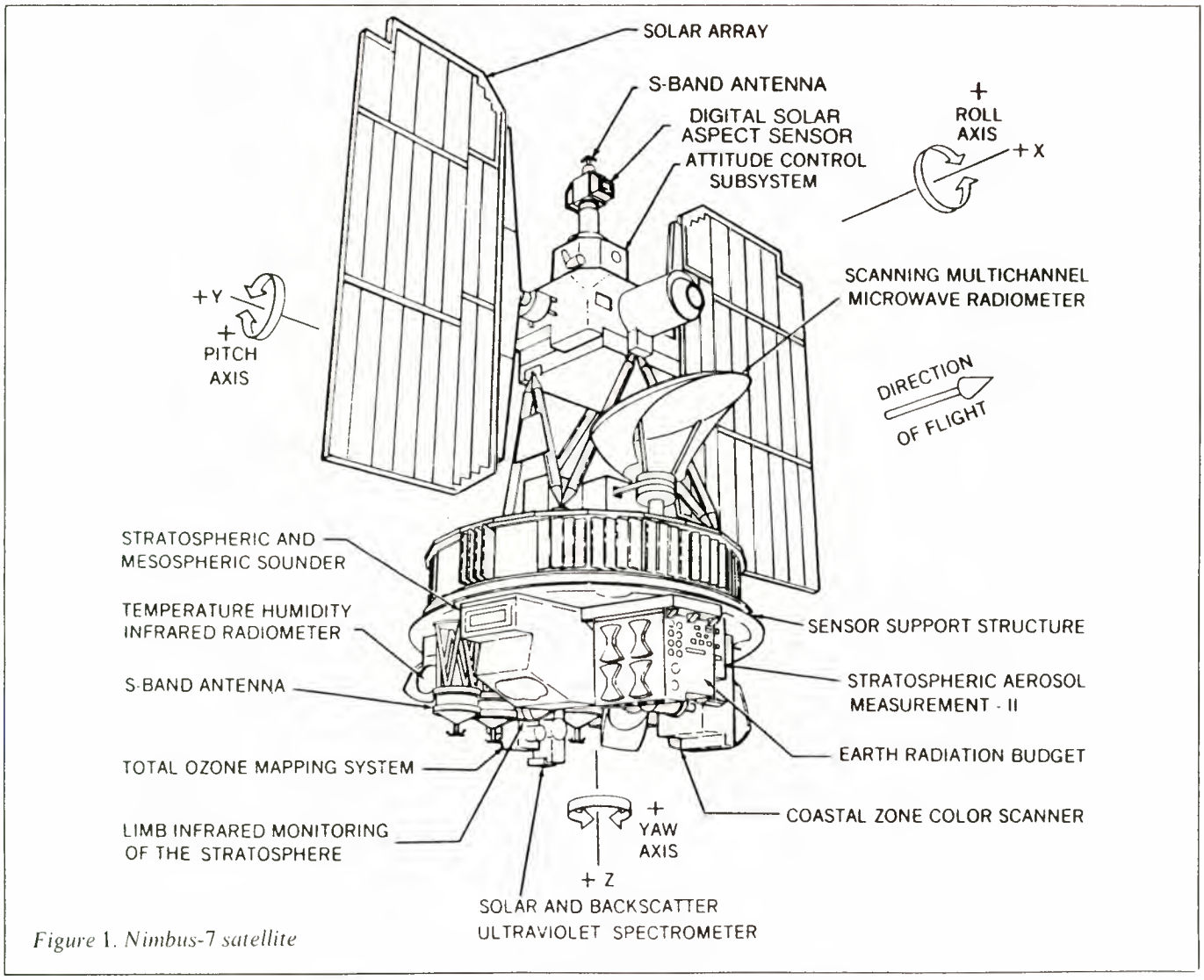

Figure 1. *Nimbus-7 satellite*

One of the instruments, the Coastal Zone Colour Scanner (CZCS), built by Ball Brothers Inc., is a six channel image scanner of high-sensitivity operating in the visible, near infrared and in the thermal infrared region of the spectrum. Its objective is to measure pigment concentration, yellow substance concentration as salinity indicator, sediment distribution and sea surface temperature (49).

a. CZCS optical system (Fig.2)
The CZCS uses a fully rotating mirror (13″ × 9″) which scans at 480 rpm (8 scans/s) orthogonal to the flight track. The mirror is arranged at 45° with reference to the telescope optical axis with the capability of being tilted by ± 20° in increments of 2° about the pitch axis to avoid sun glint.

The telescope is a F/4 standard Cassegrain configuration with 177.8 mm aperture diameter and 711.2 mm focal length. A dichroic beam splitter reflects infrared radiation through relay optics to the HgCdTe detector which is located at the radiation cooler (120 K).

Initial calibration in the visible/near infrared region is provided by a pair of tungsten lamps (redundancy), a filter for spectral shaping and a shutter for exposing the lamp once every eight scans.

b. Spectral bands
The separation of the 5 visible/near infrared channels is achieved by the use of a 600 lines/mm spherical grating (Fig. 2). The bandwidths of these channels are defined by exit slits mounted in front of the Si photodiodes in the focal plane of the spectrometer. The individual bands are listed in Table 2. The spectral bands at 443 nm and 670 nm, are centered on the most intense absorption bands of chlorophyll, while a band at 550 nm is centered on the 'hinge point', the wavelength of minimum absorption.

Table 2. Nimbus-7/CZCS spectral bands

Spectral bands	Centre	Half-widths
Visible/near IR	443 nm	20 nm
	520 nm	20 nm
	550 nm	20 nm
	670 nm	20 nm
	750 nm	100 nm
Thermal IR	11.5 m	2 m

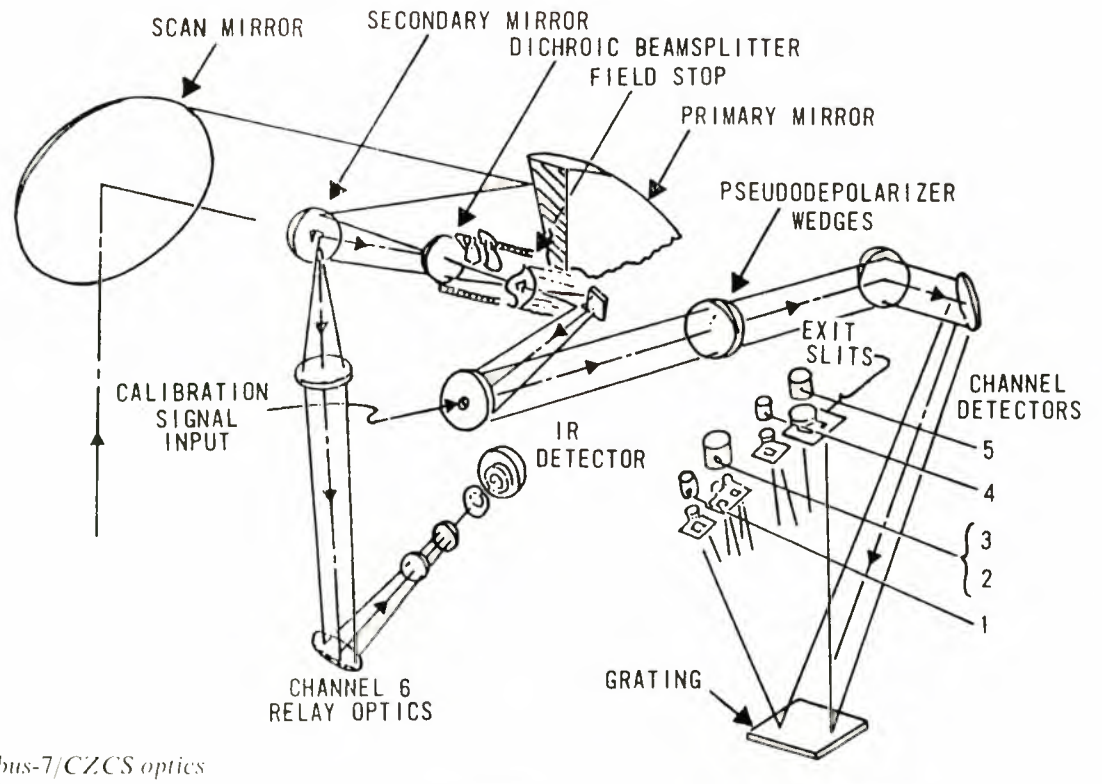

Figure 2. Nimbus-7/CZCS optics

Each of the channels 1 to 4 has selectable gain setting to allow for sun angle variations during the year. They are optimised for the albedo of water. Channel 5 has only one gain setting (the same as Landsat MSS 6) as it is for use over land.

It is adjusted for the high noon ascending node of Nimbus-7.

c. CZCS scanning geometry

The scanning geometry of the CZCS is illustrated in Figure 3. There is an overlap of 0.209 km in flight direction.

d. Present status

Since its launch in 1978, the CZCS has produced thousands of scenes which are archived and analysed in many laboratories around the world.

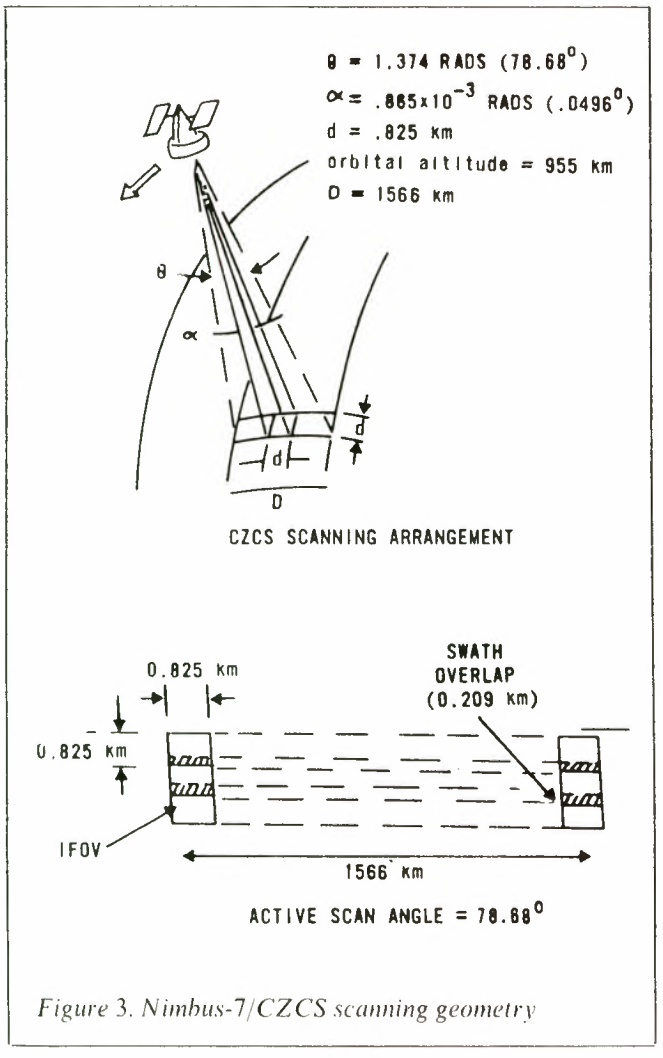

Figure 3. Nimbus-7/CZCS scanning geometry

In open ocean areas the critical atmospheric correction has been solved for certain environmental conditions. Problems remain to be solved in coastal areas.

The instrument (design life time: 1 year) is still operating but loses sensitivity steadily, especially in the blue. This causes calibration problems which are critical in regard to the atmospheric correction.

Operation of the thermal channel was terminated in late 1981 because of problems with the cooling system. NASA plans to operate the instrument at least till 1984.

1.2 *NOSS/CZCS*

The National Oceanic Satellite System (NOSS) was intended as a limited (5 years) operational demonstration of producing oceanographic data products for both, military and civilian users in near real time, based upon remote sensing from spaceborne instruments. The four principal instruments were:

- Large Antenna Multichannel Microwave Radiometer (LAMMR)
- Radar Altimeter (RA)
- Scatterometer (SCATT)
- Coastal Zone Colour Scanner (CZCS).

One of the goals of this mission was a very rapid return and processing of global data especially for the observations of wind, sea state and sea surface temperature with delays as small as three hours between observations and the transfer to users.

The CZCS on NOSS (called CZCS II) was planned to be modified in comparison to the Nimbus-7/CZCS as summarised in Table 3. The NOSS programme was deleted at the beginning of 1981.

Table 3. NOSS/CZCS specifications

IFOV		1.13 mrad
Pixel size		791 m
Radiometric resolution		10 bit
Spectral bands	Centre	Half-width
Visible/Near IR	440 nm	20 nm
	490 nm	20 nm
	560 nm	20 nm
	590 nm	20 nm
	650 nm	20 nm
	685 nm	20 nm
	765 nm	40 nm
	867 nm	45 nm
Thermal IR	10.3 – 11.3 μm	
	11.5 – 12.5 μm	

1.3 *ERS-1/CZCS*

After the deletion of the NOSS programme and after the removal of the Ocean Colour Monitor (OCM) from the ERS-1 payload (section 2.4), negotiations took place between NASA and ESA in an attempt to fly a CZCS on ERS-1.

An investigation into the technical feasibility to embark a CZCS on ERS-1 was undertaken by a joint NASA/ESA team (50). The result of this study was: 'The CZCS (improved version of the Nimbus-7/CZCS) is slightly reduced in performance but essentially similar to the OCM in its mission aims and instrument technology. In view of its longer development history and taking into account the results of the technical investigations, it can be concluded with high confidence that it could be made technically compatible with ERS-1, provided that the necessary funding for the modifications is made available.'

In spite of the general interest in this solution, this option is not further pursued at present.

1.4 *NOAA/CZCS (OCI)*

a. A re-flight of an advanced CZCS, called Ocean Color Imager (OCI) as part of the operational satellite programme is presently studied by NASA and NOAA (Fig. 4). For this purpose the orbital parameters of the spacecraft will have to be changed as listed in Table 4.

b. The instrument specifications of the OCI are summarised in Table 5. Besides the addition of further spectral channels and an increase of sensitivity (10 bit radiometric resolution) in comparison to the Nimbus-7/CZCS, the major change on the instrument side is the removal of the thermal channel since the Advanced Very High Resolution Radiometer (AVHRR) of Tiros will be used for simultaneous water temperature monitoring.

Two different data rates are envisaged:
- High data rate mode:
  10 minutes of data will be recorded or transmitted in real time.
- Low data rate mode:
  By selective sampling only every 4th pixel and 4th scan line are recorded (recording time: 160 minutes, however only 30 minutes of data above area with suitable sun angle).

Table 4. NOAA-J orbital parameters

Altitude	870 km
Orbit time	102.3 min
Separation	25.587°
Node	Ascending
Inclination	98°
Orbits/day	14
Equator crossing	1.30 PM
Re-visit	8 days

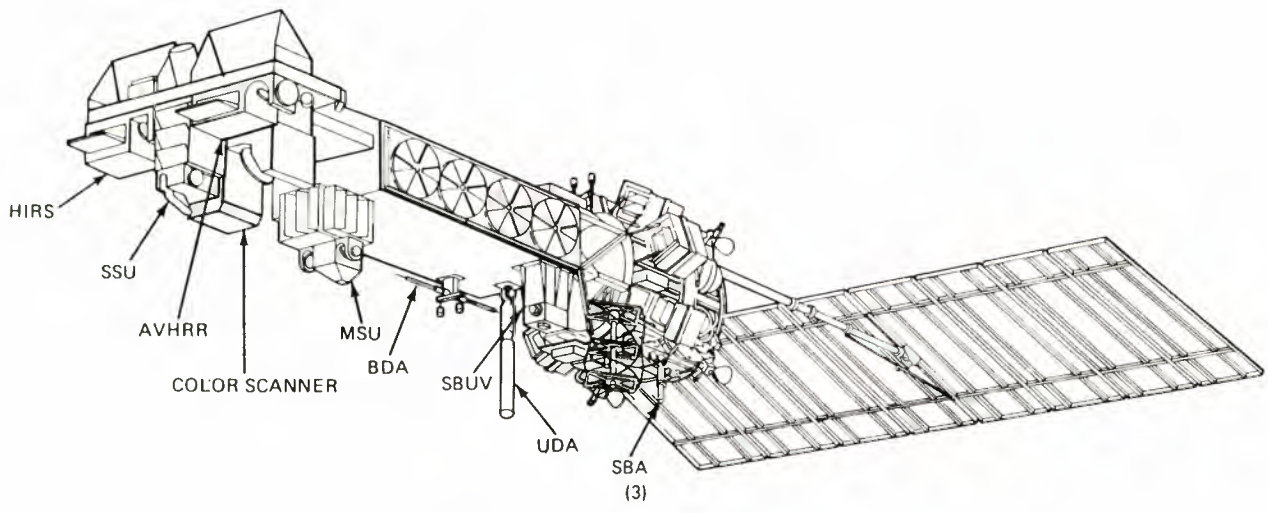

Figure 4. Color scanner on NOAA satellite

Table 5. OCI specifications

Spectral bands	Centre	Half-width
Nominal	440 nm	20 nm
	520 nm	20 nm
	550 nm	20 nm
	670 nm (660)	20 nm
	765 nm	50 nm
	865 nm	50 nm
Experimental	490 nm	20 nm
	685 nm	20 nm
Tilt	0°–20° (in less than 30 s)	

Table 6. OCE specifications

IFOV	3.5 mrad
Pixel size (nadir)	973 m
FOV	90°
Swath width (at 138 nautical miles altitude)	510 km
Radiometric resolution	10 bit

Spectral bands	Centre wavelength	Half-width
	485.9 nm	23 nm
	518.4 nm	23 nm
	552.6 nm	23 nm
	584.5 nm	23 nm
	620.6 nm	23 nm
	655.1 nm	23 nm
	685.1 nm	23 nm
	786.6 nm	52 nm

c. The incorporation of the OCI on this mission has not been approved yet, however, if this will be the case, a launch in 1986/87 is planned.

2. Ocean Colour Experiment (OCE) on OSTA-I

a. GENERAL

During the second orbital flight test of the US Space Shuttle in November 1981, six remote-sensing experiments were incorporated into the OSTA-I payload. One of these was NASA's Ocean Colour Experiment (OCE). The OCE basically consists of the Ocean Colour Scanner which was mounted in the cargo bay of the Orbiter and operated above selected portions of the world's oceans (51).

b. OCE

The instrument is an 8 channel opto-mechanical image scanner of high sensitivity, which is dedicated to the measurement of water colour. The concept of the instrument originates from pre-launch activities related to the CZCS on Nimbus-7. It was designed and built at the Goddard Space Flight Center and operated before frequently on high flying aircraft. The instrument specifications are listed in Table 6.

c. MISSION AND DATA COLLECTION

The OSTA-I mission in general, and the OCE experiment in particular, were affected to a large extent by the frequent delays in the Shuttle launch date, by the abbreviated mission duration and finally by the prevailing weather conditions, especially along the US coast.

In spite of this, the basic objectives of the experiment have been met. About one-third of the 120 minutes of data collected by the OCE are cloud free and are evaluated at present in the US and in Europe.

d. OSTA-V/OCE

In view of the restrictions during the OSTA-I mission, in particular in terms of ground truth measurements and verifications, a re-flight of the OCE on the OSTA-V mission to be launched in 1986 in combination with an extended, well-scheduled ground truth programme is presently discussed.

3. Multispectral Scanner (MSS)/Thematic Mapper (TM) on Landsat

Although the Landsat/MSS since its 10 years of operation has been used frequently for the monitoring and mapping of estuarine and coastal phenomena and especially its visual interpretation (52) the instrument is not really designed for a quantitative analysis of water constituents and large scale oceanic processes.

The situation will improve to a limited extent in the near future with the launch of the Thematic Mapper on Landsat-D later in 1982. The orbital parameters of Landsat-D are listed in Table 7. (These values are slightly different for Landsat-D′ planned as a backup).

The Thematic Mapper is a seven-band scanning radiometer operating in six solar reflected spectral bands between 0.45 and 2.35 μm and a thermal band in the 10.4

to 12.5 μm region (see Table 8). The optical design makes use of an object plane scan mirror (21″ ellipse) which permits the telescope to operate at very small field angles.

Contrary to the MSS, the TM collects data in both scan directions. A scan line corrector, which employs two small mirrors (parallel to each other, but rotating on a common axis) rotates perpendicular to the scan mirror at a rate that cancels out the forward motion of the spacecraft during each scan. This produces effectively parallel scan lines with neither overlap nor underlap.

The telescope uses a F/6 Ritchey-Chretien configuration (16″ϕ). For bands 1 to 4 high-resolution Si detector arrays (16 each) in combination with optical filters are used. As the scan mirror oscillates, 16 lines are swept out simultaneously in all bands across the 185 km swath. Cooled detector arrays which serve bands 4 to 7 in a similar way are placed at the rear of the instrument on a plate maintained at 95 K. Indium antimonide is used for bands 5 and 6 while mercury cadmium telluride is used for band 7.

Table 7. Landsat-D orbital parameters

Altitude	705 km
Orbit	sunsynchronous
Equator crossing	9.30 AM
Node	descending
Inclination	98.2°
Repeat period	16 days
Launch	1982

Table 8. TM specifications

IFOV	0.0425 mrad
Pixel size (nadir)	30 (120) m
FOV	14.9°
Swath width	185 km
Radiometric resolution	8 bit
Spectral bands	
Channel 1	0.45 – 0.52 μm
Channel 2	0.52 – 0.60 μm
Channel 3	0.63 – 0.69 μm
Channel 4	0.76 – 0.90 μm
Channel 5	1.55 – 1.75 μm
Channel 6	2.08 – 2.35 μm
Channel 7	10.4 – 12.5 μm

a. GENERAL

Generally speaking the TM will be an improvement in comparison to the MSS in view of its higher spatial and radiometric resolution and with the incorporation of a thermal channel. (The thermal channel of Landsat-C failed shortly after launch!). However, the bandwidths, the center wavelengths, radiometric resolution and swath width place most probably limitations on the application in terms of water colour monitoring.

b. COASTAL AREAS

The monitoring of typical coastal processes (e.g., sediment transport, pollution, interaction of river discharges with tidal currents, monitoring of land/water boundaries etc.) will be superior in comparison to the capabilities of the MSS. However, the repeat cycle of 16 days (without Landsat-D′) is still considered to be too long. A quantitative evaluation of relevant water constituents in coastal waters is still to be proved.

c. OCEAN AREAS

The addition of the band in the blue spectral region (channel 1) in the TM in principle opens the possibility for monitoring pigment concentrations in offshore waters. However, this will depend on the suitability of channels 4, 5, 6 to be used for the atmospheric correction of channels 1 and 2. It will further depend on the suitability of the comparatively broad channel (together with channel 2) to determine chlorophyll. A radiometric resolution of 8 bit is generally considered to be insufficient for this purpose.

4. Ocean Colour Monitor (OCM) on ERS-1

After its initial incorporation into the Coastal Oceans Monitoring Satellite System (COMSS) which is not pursued any further, the Ocean Colour Monitor (OCM) was intended as a follow-on design of the CZCS to be integrated into the payload of the first ESA Remote Sensing Satellite (ERS-1). This mission is dedicated towards oceanographic research and applications.

The OCM is a highly advanced opto-mechanical multispectral scanner of very high sensitivity, dedicated to the simultaneous (pixel by pixel) measurement of water colour, water temperature and of some atmospheric parameters. In spite of the demands of the user community, it was removed from the payload of ERS-1.

In view of the advanced experience in water colour monitoring in comparison to other technologies, the OCM and an OCM-like concept is being further investigated for incorporation into future missions. Its present configuration is shown in Table 9.

Special design features of the ERS-1/OCM incorporate 4 detectors for each channel and a co-registration between individual channels within ± 0.1 pixel. Furthermore a high signal/noise ratio and the exceptional good calibration of 0.1% (relative) and 2% (absolute) in the visible range, 0.1 K (relative) and 0.5 K (absolute) in the thermal channels should be mentioned.

The orbital parameters of ERS-1 (after raising its altitude) are listed in Table 9a.

5. Multispectral Electronic Self-Scanning Radiometer (MESSR) on MOS-1

a. GENERAL

The Japanese Maritime Observation Satellite I (MOS-1) will be launched in 1987 and incorporates the following remote sensing payload:

- Multispectral Electronic Self-scanning Radiometer (MESSR)
- Visible/Thermal Infrared Radiometer (VTIR)
- Microwave Scanning Radiometer.

The orbital parameters of the satellite are listed in Table 10.

b. MESSR

While the VTIR consists of an opto-mechanical scanning system of the conventional type – pixel size: 900 m (vis.), 2700 m (thermal IR) – the MESSR is a four-channel multispectral scanner incorporating CCD arrays for monitoring simultaneously two strips of 100 km each adjacent to the nadir track. The characteristics of the instrument are summarised in Table 11 (53).

Expected Performance
Similar to the Landsat/MSS, the MESSR is expected to permit a semi-quantitative monitoring of typical coastal processes in the visible/near infrared region.

The addition of a thermal scanner on the same platform (VTIR) similar to the one on Landsat-C, is certainly an advantage if the sensitivity is high enough in regard to the subtle SST changes. The exact correlation of pixels collected in the VTIR with those collected by the MESSR will place a burden onto the ground segment.

In regard to a quantitative evaluation of water constituents, especially of pigments, the MESSR in the described configuration (50) is most probably unsuitable.

Table 9. ERS-1/OCM specifications (for more details see Annex 2)

IFOV		1.185 mrad
Pixel size		920 m
FOV		80°
Radiometric resolution		10 bit
Spectral bands	Centre	Half-width
Visible/Near Ir	400 nm	20 nm
	445 nm	20 nm
	520 nm	20 nm
	565 nm	20 nm
	640 nm	20 nm
	685 nm	20 nm
	785 nm	30 nm
	1020 nm	60 nm
	1600 nm	100 nm
Thermal IR	3700 nm	400 nm
	8500 nm	500 nm
	10800 nm	1000 nm
	12000 nm	1000 nm

Table 9a. ERS-1 orbit specifications

Altitude	770 km
Inclination	98°
Node	descending
Equator crossing	noon
Re-visit time	3 days

Table 10. MOS-1 orbit specifications

Altitude	909 km
Orbit	sunsynchronous
Re-visit time	17 days
Orbit time	103 mn

Table 11. MOS-1/MESSR specifications

Pixel size		50 m
Swath width		2 × 100 km
Radiometric resolution		6 bit
Spectral bands	Center	Half-width
	550 nm	80 nm
	650 nm	80 nm
	760 nm	80 nm
	950 nm	300 nm

The bandwidths of channels 1 and 2 are too wide, there is no blue channel (chlorophyll absorption band), the radiometric resolution of 6 bit is too small. Further, in regard to the study of large scale phenomena, the swath width is too small; the repeat cycle is not fast enough.

6. High-Resolution Visible Sensors (HRV) on SPOT

a. SPOT PAYLOAD

The payload for the SPOT (Système Probatoire d'Observation de la Terre) satellite to be launched in 1985 includes two identical High-Resolution Visible Sensors (HRV) which are able to acquire images of earth surface in visible and near infrared wavelengths.

The two instruments have elementary fields of view of 10 m or 20 m and a swath width of 60 km (for vertical viewing) each. A 4 km overlap between the two instruments allows a global field of view of 116 km in nadir position.

A pointing mirror in front of each instrument allows offset pointing of $\pm 27°$ around the roll axis of the spacecraft. This capability enables the acquisition of stereoscopic images from several orbits with different aspect angles, and increased accessibility over selected areas (i.e., a lower time delay between two successive images of the same area) (Fig. 5).

Each of the two HRV sensors can operate in the multispectral mode and/or in the panchromatic mode (Table 12).

Images are obtained using the push-broom technique. This is done with a suitable linear array of detectors located in the focal plane of the instrument. A ground resolution of 20 m (pixel size) over a 60 km swath requires an array of 3000 detectors.

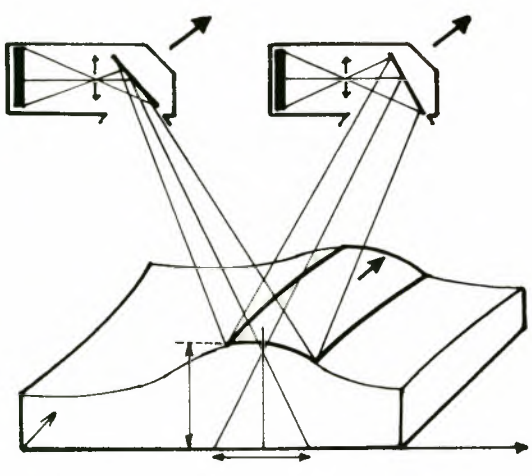

Figure 5. SPOT/HRV stereoscopic operation

The orbit parameters of the SPOT satellite are listed in Table 13.

b. EXPECTED PERFORMANCE

For the investigations above water, the advantage of the HRV instruments lies in the high geometric resolution capability rather than in radiometric of thematic performance.

Coastal waters: The high geometric resolution will permit an accurate monitoring of land/water boundaries and also an improved (in comparison to the MSS) monitoring of sediment transport in estuaries and coastal zones.

The short repeat period (5 days with tilting) is of advantage for coastal monitoring but not enough for tidal studies.

Open ocean areas: A quantitative evaluation of pigment concentration will most probably not be possible with the HRV because no blue channel is included, the radiometric resolution is not high enough and an atmospheric correction by the aid of channel 3 will be insufficient. For the monitoring of large scale features the swath width is too low. However, again the repeat frequency of 5 days (by tilting) is of advantage for the monitoring of small scale dynamic features.

Table 12. SPOT/HRV sensor specifications

Multispectral mode		
Pixel size		20 × 20 m
Swath width		60 km (each)
Spectral bands	Centre	Half-width
	545 nm	90 nm
	640 nm	80 nm
	845 nm	110 nm
Panchromatic mode		
Pixel size		10 × 10 m
Swath width		60 km (each)
Spectral bands	Centre	Half-width
	545 nm	90 nm

Table 13. SPOT orbit specifications

Altitude	822 km
Inclination	98.7°
Node	descending
Equator crossing	10.30 AM
Re-visit time	26 days
Orbit time	101 mn

Annex 2
Experiment Interface Document
Ocean Colour Monitor (OCM)

(As proposed for ERS-1 Phase B study activities)

1. OCM Description

The OCM is a mechanical scanning radiometer operating both in the visible/near IR and thermal IR part of the electromagnetic spectrum.

The major objective of the OCM is to provide a simultaneous mapping of sea constituent concentrations such as phytoplankton, yellow substance with sea surface temperature gradients.

The number of spectral channels, 13, and their characteristics (wavelength position, bandwidth) will make this a powerful instrument for ocean monitoring.

The spectral focal plane separation provides interchannel registration to allow multispectral pixel creation and processing.

The cooling of IR detectors is foreseen by the use of some mechanical cooler such as the ATSR.

Calibration for the visible channels is based on original concept which uses a diffuser glass, and for IR channels, the calibration source is a combination of a black body and space viewing.

2. OCM Channel Specifications

Based on the 777 km orbit altitude and for a pixel of 800 m, the radiometric and geometric specifications of the different spectral channels are given here after.

IFOV = 10.3×10^{-4} rad – Total FOV = ± 40

MTF 0.4 and $f_N = \frac{1}{2}$ = 422 cycles/rad

Calibration

	Visible	*IR*	
relative	0.1%	0.1 K	290 K
absolute	2.0%	0.5 K	

Image quality
Pixel size 10.3×10^{-4} rad
Equi-angularity within 0.1 pixel
Spectral channels: co-registration within ± 0.1 pixel
Pixel localisation ± 0.5 pixel
Stability ± 0.1 pixel

3. OCM Functional Block Diagram and Optical Scheme (see page 48).

4. Mechanical Interfaces

4.1 *Drawing*
The architectural concept and the overall dimensions of the OCM are presented on page 49.

Spectral, radiometric, spatial resolution

no.	λc (nm)	$\Delta\lambda$ (nm)	$NE\Delta\rho$ / $NE\Delta T$ $\theta_s = 60°$	$\Delta \times$ (m)	Comments
1	400	20	$< 10^{-3}$	800	Yellow substance
2	445	20	$< 5 \times 10^{-4}$	800	First priority chlorophyll
3	520	20	$< 5 \times 10^{-4}$	800	Chlorophyll/Turbidity
4	565	20	$< 5 \times 10^{-4}$	800	Turbidity
5	640	20	$< 5 \times 10^{-4}$	800	Turbidity/baseline fluo Cla
6	685	20	$< 5 \times 10^{-4}$	800	Chlorophyll fluorescence
7	785	30	$< 5 \times 10^{-4}$	800	Atmospheric correction
8	1020	60	$< 5 \times 10^{-4}$	800	
9	1600	100	$< 5 \times 10^{-2}$	800	Water/Ice clouds
10	3700	400	< 0.17 K	800	Day/Night sea-surface
11	8500	500	< 0.12 K	800	temperature
12	10800	1000	< 0.12 K	800	and atmospheric
13	12000	1000	< 0.12 K	800	corrections

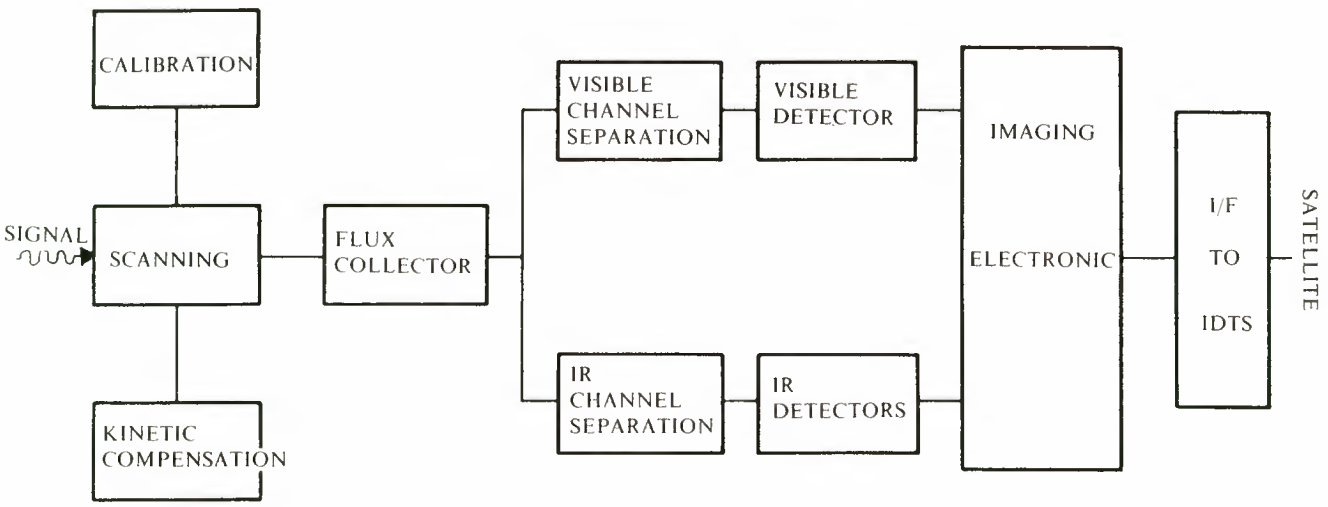

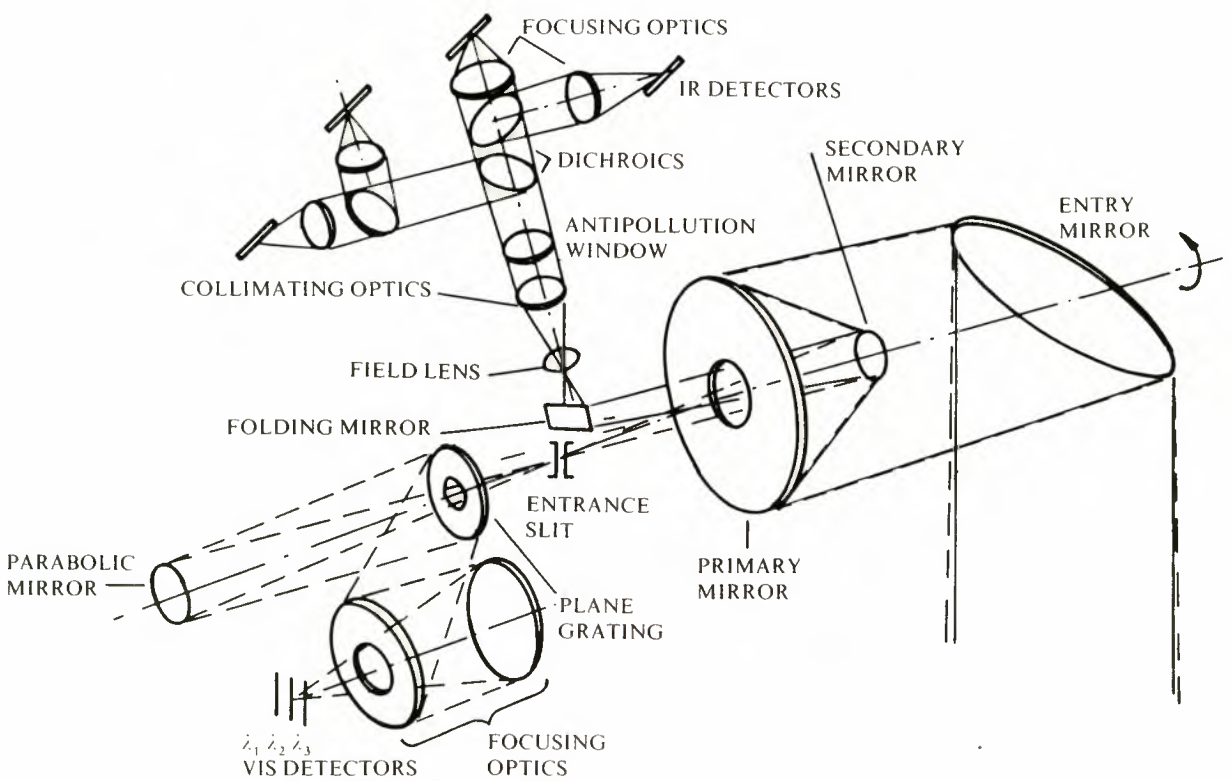

OCM FUNCTIONAL BLOCK DIAGRAM AND OPTICAL SCHEME

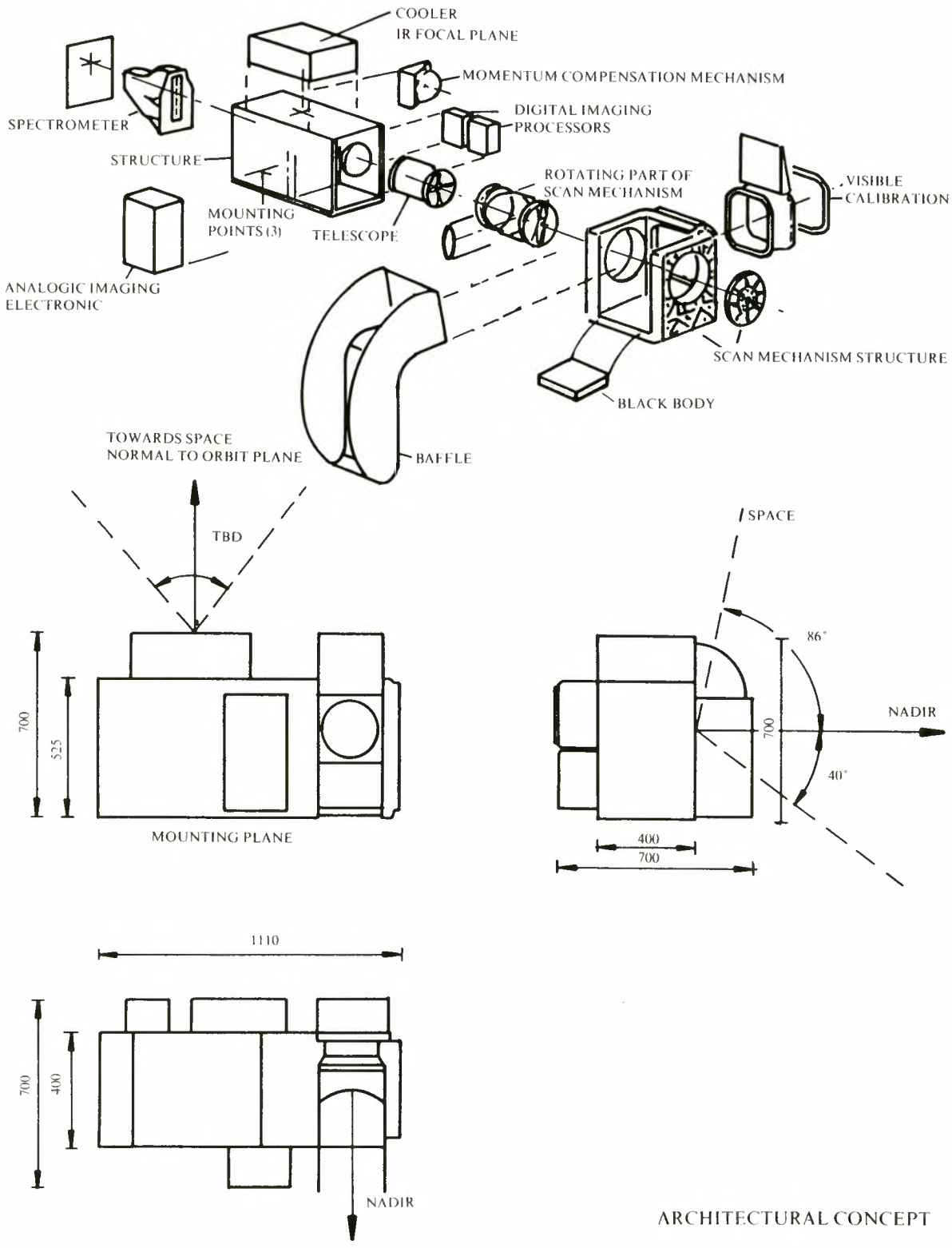

ARCHITECTURAL CONCEPT

4.2 *Fixation*
Fixation is realised with 3 mounting points.

4.3 *Alignment*
Alignment requirements are within 0.25° of the satellite reference axes. Position of OCM axes (defined by optical cube) with respect to satellite axes will be measured with ±0.1 accuracy.

Variation after launch within 0.15.

4.4 *Mass breakdown*

Scanning mechanism + kinetic compensation	8 kg
Telescope + Visible for IR separation	8
Calibration	3
Functional electronics	5
Imaging electronics	15
Structure	16
Thermal control	10
	65 kg

4.5 *Dynamic characteristics*
Compatible with document (ref. 'Plate-forme Multi-mission – Manuel de l'Utilisateur').
- Kinetic momentum < 1 Nms
- For F < 0.2 Hz payload creates:
  no kinetic momentum > 1 Nms
  no torque > 5×10^{-2} Nm
  Payload natural frequencies < 2 Hz and > 8 Hz.

4.6 *Connectors location*
TBD.

5. Thermal Interfaces

The OCM is as much as possible thermally decoupled (conduction and radiation) from payload and PFM.

Radiative decoupling will be realised by multilayer super insulation and baffles when necessary.

Passive and active thermal control techniques will be used.

IR detector will be cooled with a mechanical cooler.

Heaters for black body calibration temperature, for IR optics decontamination, or instrument temperature uniformity are TBD.

One side is viewing space for thermal dissipation of power dissipated from the mechanical cooler.

Free field of view is TBD (nominally as for the ATSR).

Emissivity and absorptivity of external surface TBD.

6. Electrical Interfaces

6.1 *Electrical scheme*
The electrical concept is presented in the following drawing: (see next page)

6.2 *Power consumption*
All power consumption figures are from the 28 V spacecraft unregulated bus except for a minimum power (TBD) from the 50 V regulated for ITU.

Equipment	Power consumption			Operating mode
Active thermal control	25 W			Permanent
Active cooling	35 W			Permanent
Functional electronics				
• Command and control	5			Permanent
• Power stages	8			Permanent
• Miscellaneous electronics	1			Permanent
Image channel electronics	A	B	C	
Visible detector preamp.	2.4	0		
IR preamp.	6.6	6.6		
Analog signal processing	60	20	2	
Digitial signal processing	13	13		
	A	B	C	
Total	156	113.6	76	

A = 1/2 orbit in day-time
B = 1/2 orbit in night-time
C = stand-by for short durations (< 1 orbit)

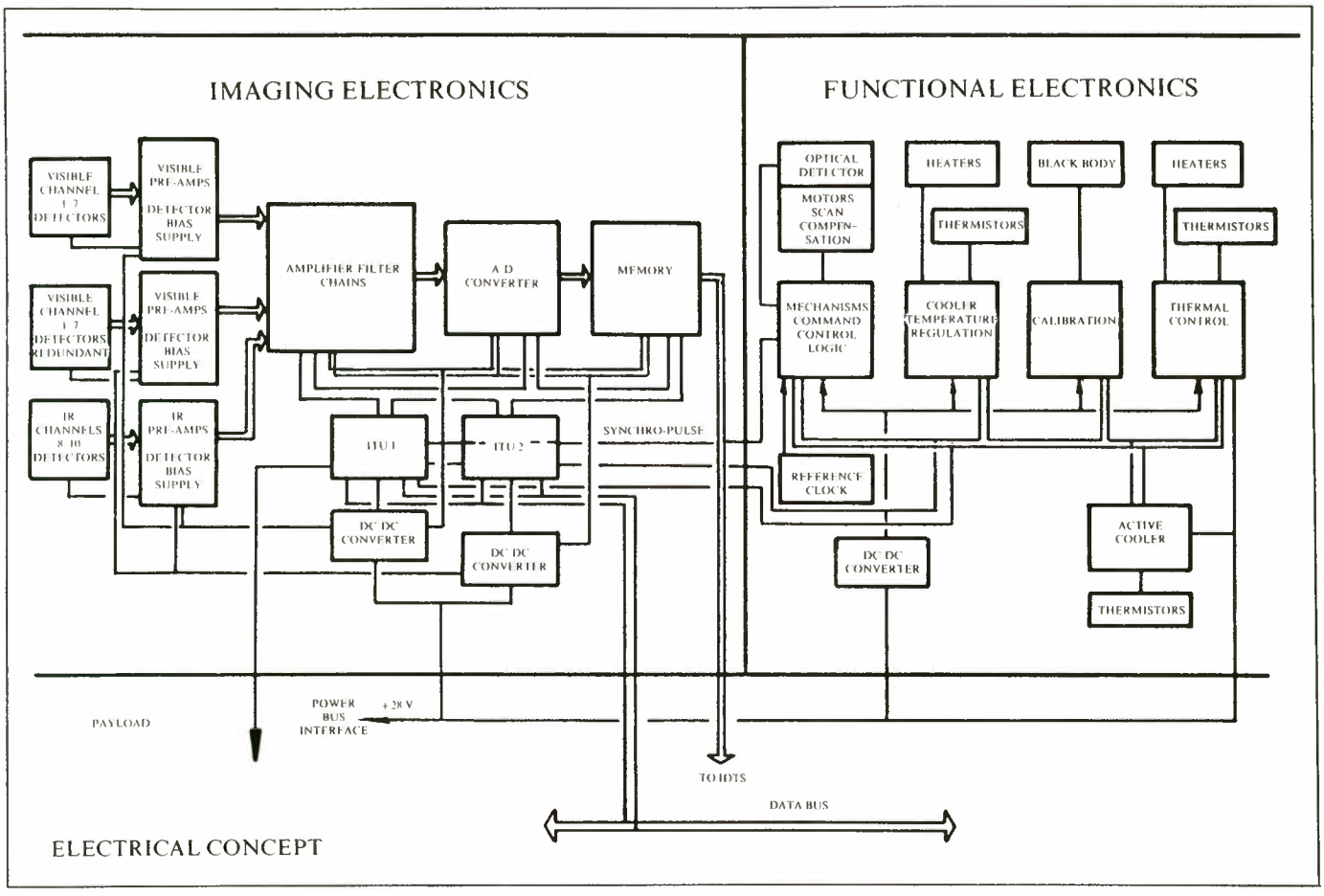

6.3 *Pyrotechnics*
TBD.

6.4 *IDTS interfaces*
- Data
  Digital data are 12 bits parallel words.
  Maximum data rate with all the channels is 2.1 Mb/s.
  During night-time useful data rate is $2.1 \times \frac{8}{13}$ 1.3 Mb/s.
  OCM has its own internal clock/synchronisation signal.
  Time data in the format is required.

6.5 *Telemetry*
Up to 80 analogue channels and single bit status are required.

Sampling rate TBD.

6.6 *Telecommands*
Up to 80 single pulse relay commands for power/status switching are required.

7. Cleanliness

7.1 *Magnetostatic*
The instrument will have a motor driver for the scanning mechanism, another one for the active cooler, and a magnetic bearing.

7.2 *Electrostatic*

7.3 *Electromagnetic*

7.4 *Chemical* (similar to the TBD requirements for the ATSR)
Optical surfaces are sensitive to particles, water condensation, hydrocarbon, hydrazine.

Contamination controls and decontamination procedures shall be established.

Outgassing
Material will be selected from ESA approved list.

Annex 3
OCM-CZCS Comparison

The following figures attempt to illustrate the significant technical improvements that the mechanical scanning OCM can offer with respect to the CZCS-2. The CZCS-2 represents an improvement of the CZCS as flown on Nimbus-7. These improvements are in the area of spectral band selection and numbers. The basic instrument design, in terms of dimensions and working principle has not been modified.

Figure A3.1 indicates the main parameters necessary to compare the instruments' performances. Figures A3.2 and A3.3 compare the spectral bands proposed and their associated S/N (signal to noise ratio) for the visible and very near infrared channels. The CZCS figures are those proposed by NASA. Figure A3.4 shows that a theoretical analysis for channel 2 based on the telescope diameter and number of detectors for each band leads automatically to the conclusion of superior performance for the OCM. Figure A3.5 provides a similar comparative performance for the thermal infrared channels.

An important aspect of the OCM is the utilisation of a 'split window' for the 10–12 μm band which together with the 3.7 μm band provides for a much improved sea surface temperature recovery compared to the CZCS.

Finally, Figure A3.6 gives a more general technical comparison of the two instruments.

Figure A3.1. OCM/CZCS-2

Electrical Signal
- Pupil diameter ϕ (m)
- Pixel size d (m)
- Orbit altitude H (m)
- Spectral detector sensitivity $R\lambda$(A/W)
- Spectral optical transmission τ_λ
- Spectral radiance from pixel
  L_λ (w . m^{-2} . sr^{-1} . μm^{-1})
  geometric conditions $\theta_s, \theta_r, \varphi$
  atmospheric quality
- Spectral bandwidth $\Delta\lambda$ (μm)

Noise
- Electrical bandwidth (number of detectors)
- Signal fluctuations
- Electronic noise (preamp.)
- Encoding noise
- EMC noise (margin)

Figure A3.2 OCM/CZCS-2

THEORETICAL PERFORMANCE COMPARISON OF OCEAN COLOUR MISSION

OCM (S/N over ocean for $\theta_s = 60°$, $\theta_r = 51°$)

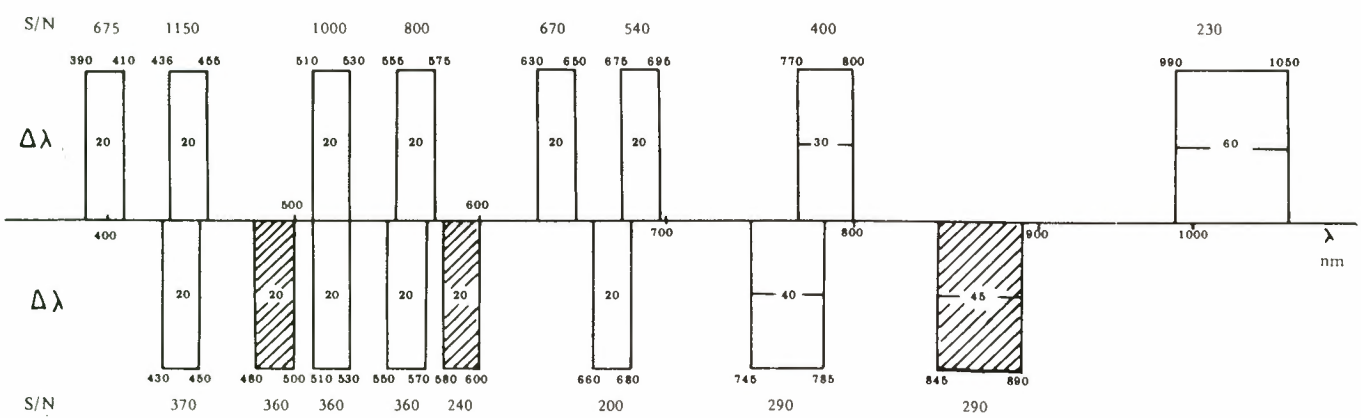

CZCS-2 (S/N calculation conditions not known, except $\theta_s = 60°$)

corresponds to new channels compared to CZCS-1

Figure A3.3. OCM/CZCS-2

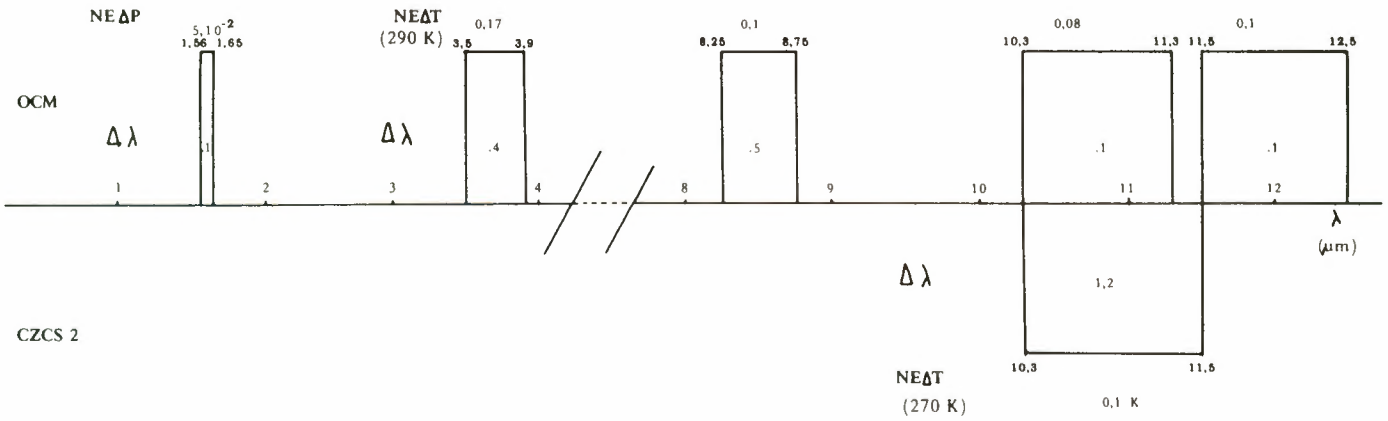

Figure A3.4. OCM/CZCS-2

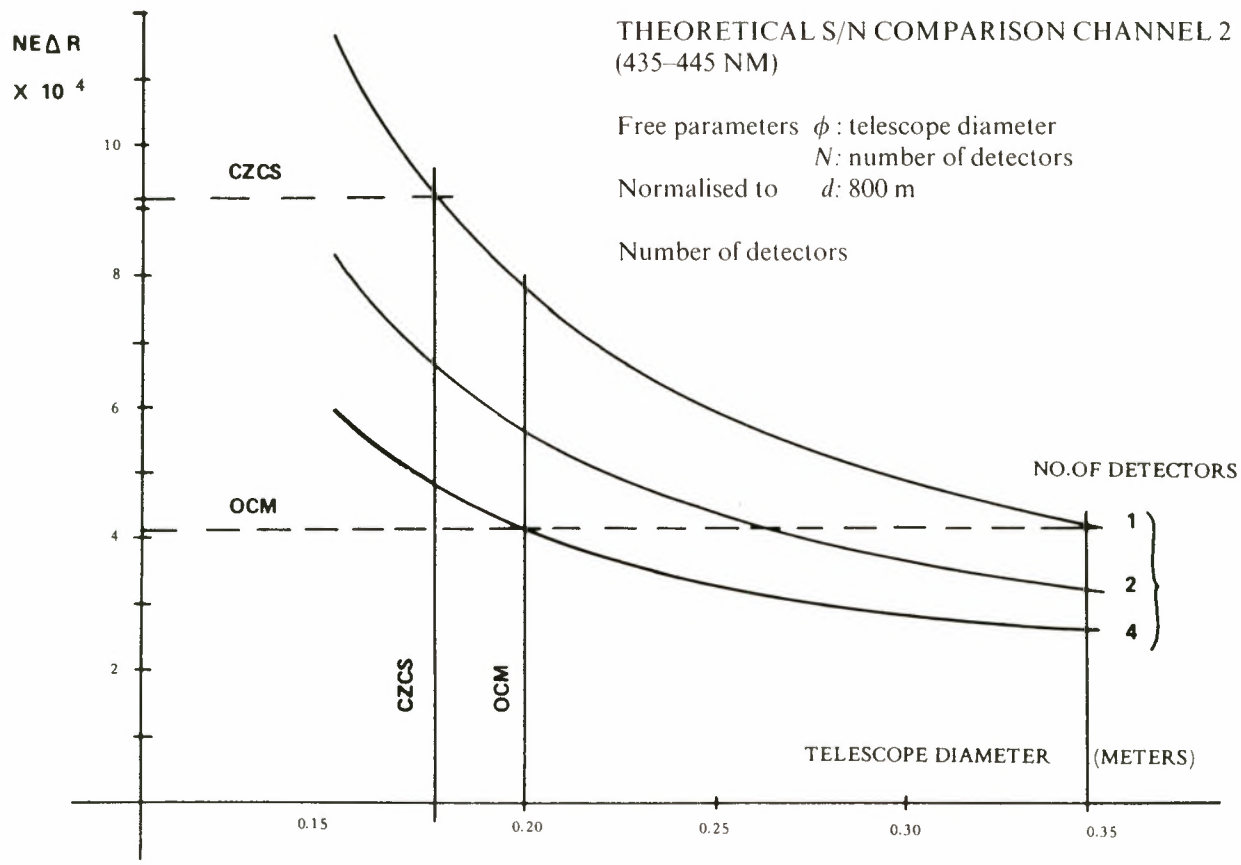

Figure A3.5. OCM/CZCS-2

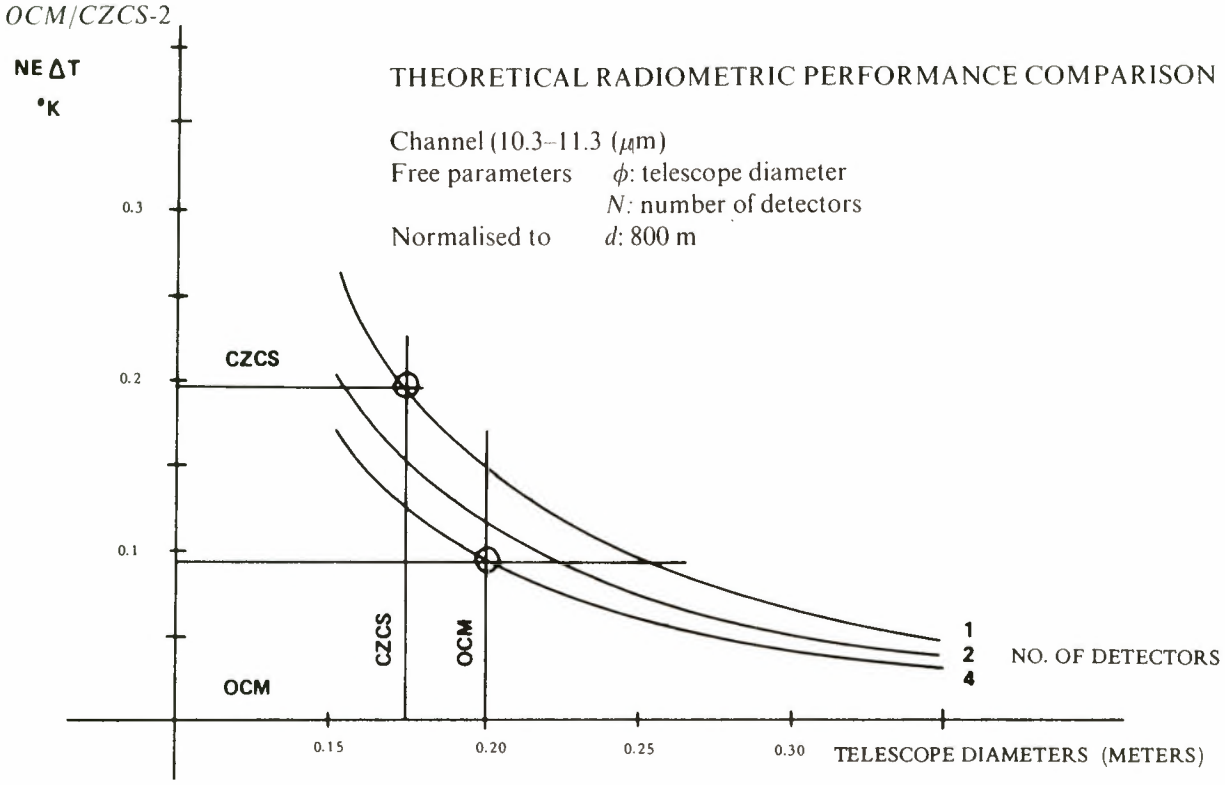

Figure A3.6. OCM/CZCS comparison

Parameters	CZCS-2	OCM	Comments
Channels	Visible 7 IR 1	Visible 8 Mean IR 1 IR 4	CZCS mini-configuration 5 channels
IFOV Footprint	1.13 mrad 791 m	1.185 mrad 800 m	
Swath	40°	40°	1300 km
Scan-rate	8.53 Hz	2.13 Hz	Contiguous at nadir OCM 4 detectors/channel
Sample rate	1.12/IFLOV	1.2/IFOV	Cross-track
Digitisation	10 bits	12 bits	no gain change along orbit for OCM
Data-rate	max 5.3 Mbps buffered 1.2 Mbps	max 8.4 Mbps buffered 2.1 Mbps	
Sun-glint avoidance	Tilting ± 20°	Orbit phasing Specific spectral channel	
Volume	40 × 85 × 60	max 130 × 90 × 50	Comparison condition not clear.
Weight	50 kg	100 kg	Thermal, structure, D/C converter, data handling, functional electronics, momentum compensation, etc.
Power consumption	Peak 85 W Average 60 W	max 120 W	

Annex 4
Algorithms Development

The analytical algorithms (see section 2.2 'Physics of Ocean Colour') as well as a method which would rest upon eigenvector analyses (see section 2.4) are still tentative approaches. They intend to demonstrate that, beside the empirical algorithms now in use for the CZCS imagery, other methods could be developed if sensors with increased capabilities (number and position of channels, radiometric accuracy, etc.) become available in the near future.

The empirical algorithms are mainly of the type $M = A(r_{ij})^B$. They have been obtained through statistical studies of the relationships between a marine parameter M and a ratio r_{ij} of reflectances – or radiances – at two wavelengths λ_i and λ_j; M may be the pigment concentration C (chl a + pheo a, mg/m^3), or the total suspended seston S (g/m^3, dry weight), or the diffuse attenuation coefficient K/m for a given wavelength (actually the parameter M which is studied is $K-K_w$, where K_w represents the contribution of 'pure' sea water). A table of the various algorithms proposed by different authors is provided in reference 17 or in reference 36. It is obvious that, if several marine parameters (C,S or $K-K_w$) can be expressed through power laws with respect to the same r_{ij}, these parameters are necessarily and univocally linked. Such a situation is that of Case 1 waters and a general consensus tends now to appear concerning the algorithms to be used with the CZCS bands for the retrieval of C (or equivalently of S or $K-K_w$).

Recent developments address the problem of a better atmospheric correction through the use of the clear oligotrophic water radiance concept, associated with the computation of the 'normalised' water-leaving radiance (references 37,17,38). Such a method allows the spectral

Table 1. *Algorithms proposed by various investigators and having the form* $M = Ar_{ij}^{\ B}$ with $r_{ij} = L_u(\lambda_i)/L_u(\lambda_j)$ or $r_{ij} = R(\lambda_i)R(\lambda_j)$ for algorithms (2) to (5). When generating algorithms (18) and (19), data for $E_u(\lambda_i)/E_u(\lambda_j)$ and $L_u(\lambda_i)/L_u(\lambda_j)$ have been pooled.

Pigment algorithms: $M = C =$ (Chl a + Phaeo a) concentration (mg/m^3)

	λ_i	λ_j	A	B	r^2	Authors
(1)	443	550	0.50	−1.27	0.98	Gordon-Clark (1978-80)
(2)	440	560	1.62	−1.40	0.76	Morel (1978-80) (Case 1 + Case 2)
(3)	440	560	1.92	−1.80	0.97	Morel (1978-80) (Case 1 only)
(4)	443	550	1.73	−2.04	0.94	Bricaud-Morel (1983) (Case 1 only)
(5)	520	550	2.51	−6.38	0.91	Bricaud-Morel (1983) (Case 1 only)
(6)	443	550	0.78	−2.12	0.94	Smith-Wilson (1981)
(7)	443	550	0.77	−1.33	0.91	Clark (1981)
(8)	443	520	0.55	−1.81	0.87	Clark (1981)
(9)	520	550	1.69	−4.45	0.91	Clark (1981)
(10)	520	670	43.85	−1.37	0.87	Clark (1981)
(11)	443	550	1.13	−1.71	0.96	Gordon & al. (1982) (Case 1 only)
(12)	520	550	3.33	−2.44	0.93	Gordon & al. (1982) (Case 1 + Case 2)
(13)	443	550	2.45	−3.89	0.61	Sturm (1980)
(14)	443	550	0.30	−1.86		Nykjaer, Schlittenhardt & Sturm (1984)

Seston algorithms: $M = S =$ seston concentration (g/m^3)

(15)	440	550	0.398	−0.88	0.92	Clark & al. (1981)
(16)	440	520	0.331	−1.09	0.94	Clark & al. (1981)
(17)	520	550	0.759	−4.38	0.77	Clark & al. (1981)

'K' algorithms: $M = (K_{490} - 0.022)$ (18)
or $M = (K_{520} - 0.044)$ (19) (per metre)

	λ_i	λ_j	A	B	r^2	Authors
(18)	443	550	0.088	−1.491	0.90	Austin-Petzold (1981)
(19)	443	550	0.066	−1.398	0.995	Austin-Petzold (1981)

Revised and adapted from references 17 & 36.

effect of the aerosol scattering (i.e. the Ångström exponent) to be estimated at least over certain oligotrophic zones of the image (instead of being assumed). By using a model of the spectral reflectance developed for Case 1 waters only (39) a generalisation of the above concept is achievable and renders possible the estimate of the Ångström exponent not only in case of oligotrophic waters, but also in case of moderate chlorophyll concentration (40). In addition, the computation of the normalised radiances, followed by a comparison with the normalised radiances for varying C concentrations as provided by the model for Case 1 waters, provides a tool for discriminating between Case 1 and sediment-dominated Case 2 waters. Thus the algorithms, valid only for Case 1 waters, can be meaningfully used within the zones where Case 1 waters are indubitably present, whereas they are no longer erroneously used in turbid waters. For these turbid waters, the sediment load can be visualised by the changes in the normalised radiances at 550 nm (40) or by the use of specific algorithms, practically unaffected by the changes in pigment concentration, as developed for some areas (41).

Algorithms based on an underwater radiative transfer model can be developed if supported by the knowledge of the (local) absorption and scattering signatures of the diverse water types. Relevant data are being currently acquired at several laboratories.

Annex 5

ESA Activities in Technology for Optical Remote Sensing

Introduction

This annex briefly outlines the various technology investigations which the Agency has undertaken for RS optical instrumentation. This work has been performed either within the context of the RSPP or the Agency's general technology programme or, in certain incidences, jointly. The list of activities does not include areas of general engineering which may be applicable to specific instruments, or planned activities within the general technology programme which have not yet been initiated.

The listing of activities is broken down into five general areas:

1. Opto-mechanical scanning
2. Opto-electronic scanning
3. Calibration
4. Cryogenic cooling
5. On-board data processing.

1. Opto-mechanical Scanner Technology

The following activities were initiated to support the original design concept. All have been terminated following the OCM descoping from ERS-1.

1.1 *Mechanical Bearing Evaluation*
Objectives: Evaluation of breadboard bearing/shaft assembly to meet OCM requirements ($\delta\omega/\omega \sim 10^{-5}$). Develop shaft encoder to permit performance evaluation.

Results: Lubrication problem not solved. Encoding technique available.

1.2 *Magnetic Bearing Studies*
Objectives: Study of feasibility of a magnetic bearing assembly for OCM scanning.

Results: A hybrid concept. Breadboarding effort stopped.

1.3 *Study of OCM Image Scanning Geometry*
Objectives: OCM scanning/image processing trade-offs.

Results: Sun-glint avoidance (cf. CZCS) requires high data processing overhead. Optical de-rotator would add to complexity. Processing and archiving dimensions evaluated.

1.4 *Study OCM Focal Plan Optics*
Objectives: Determine preferred FPA for OCM.

Results: Preferred concept selected. Interface parameters for passive cooler and visible detectors established.

1.5 *Monolithic IR Pre-amp Technology*
Objectives: Establish technological feasibility.

Results: Feasible but expensive.

1.6 *OCM Image Electronics Breadboarding*
Objectives: Breadboard verification of OCM video channel concepts.

Results: Thick-film hybrid pre-amps for visible. Updated Meteosat IR pre-amps. Digital control for DC offset, gain matching and gain calibration demonstrated. A/D conversion methods investigated and not critical. Feasibility of design manufacture is demonstrated.

1.7 *Visible Detector Array Study and Breadboard*
Objectives: To investigate the technological feasibility to integrate the visible/near IR detectors on a single chip.

Results: Preferred technology identified. Technology samples in fabrication (European sources). A double chip may be advantageous for λ_r optimisation.

1.8 *3.7 μm Detector Study*
Objectives: Determine preferred detector (performance/cost trade-off) from CMT and InSb technology.

Results: CMT preferred for cost/complexity reasons. Performance not verified (open question).

2. Opto-electronic Scanner Technology

This section considers work performed in support of the LASS OII (visible) and OII (IR) concepts. Parallel activities in Europe are, for example:

- CCD matrix arrays for star-mappers
- CCD linear arrays for star-sensors and sun sensors
- SPOT HRV
- MBB MOMS activities
- Various imaging tubes

2.1 *Survey of TDI Devices*
Objectives: Determine availability of suitable devices as an alternative/improvement to OII baseline concept.

Results: Two commercial sources only. Only one in suitable architecture for potential OII use.

2.2 *Evaluation of Fairchild TDI Samples*
Objectives: Procedure and evaluate TDI samples.

Results: Not very encouraging for photometric applications (linearity problems).

2.3 *Survey of European and Canadian CCD Supply Potential*
Objectives: Identify the most promising potential source of CCD's for the OII requirements. Determine general industrial orientation/motivation, etc.

Results: Three potential sources with ESAT (University of Leuven) offering the best potential for custom-built devices.

2.4 *Development of CCD Focal-plane Array Technology*
Objectives: Develop precision multi-array packaging techniques (± 1 μm in all axes). Evaluate ESAT technology for potential space qualification.

Results: Work completed with promising results.

2.5 *Development of Large-Scale Linear Array Technology for Medium IR*
Objectives: Demonstrate feasibility of a 1024 element array for 1.5–2.5 μm detection at minimum operating temperature of 110 K.

Results: Objectives achieved. Possibility to manufacture and flight qualify an aircraft near-IR camera is under investigation.

2.6 *Development of the OII (IR) Focal Plane Array and Electronics*
Objectives: Design and breadboard a complete half-plane array (6 × 1024 detectors) with all interconnects and interface compatible with a passive coder. Design and breadboard imaging electronics.

Results: Design complete. Tooling available. Final phase being re-defined in view of a possible aircraft camera (see also 2.5).

2.7 *Breadboarding of OII (visible) Telescope*
Objectives: To demonstrate that requirements are technically feasible at reasonable cost. Provide data on lens mounting and thermal properties.

Results: All requirements met and exceeded. Breadboard item demonstrated to be space qualifiable.

2.8 *Design and Breadboard High-Speed Multiplexer and A/D Converter*
Objectives: Design, manufacture and test hybrid multiplexer and 2 Mbps. A/D converter module.

Results: A device of 80 g, 2 W dissipation with linearity better than 7 bits.

3. Calibration Studies

3.1 *Study of Calibration Techniques*
Objectives: Review all current visible calibration techniques used in photometry. Recommend a suitable technique for OCM/OII.

Results: Use of solar diffuser and relative calibration photometer.

3.2 *Study of Diffusers and Calibration Photometer*
Objectives: Determine diffuser characteristics to indicate the most promising material types. Consider the configuration of the calibration photometer.

Results: Encouraging initial data available. Experimental proposal for EURECA.

3.3 *Sensitivity Modelling of OCM Calibration*
Objectives: Initiate a numerical model to permit parametric analysis.

Results: Work completed but not exploited (lack of OCM funding).

4. Detector Cryogenic Cooling

4.1 *Design Study of a Passive Cooler*
Objectives: A passive cooler for ERS-1 orbit with maximum similarity for OCM & OII (IR) requirements.

Results: Task completed and critical technology items identified.

4.2 *Breadboarding Critical Passive Cooler Items*
Objectives: Technology investigations of fabrication techniques.

Results: On-going.

4.3 *Evaluation of Oxford/RALStirling Cycle Cooler*
Objectives: Evaluation of this UK-funded item for OCM and other applications.

Results: On-going.

5. On-board Image Data Processing

5.1 *Image Data Reduction and Compression*
- Study of ERS data reduction unit
- Multispectral Image Encoding
- Image Sensor Processing

5.2 *On-board High-Speed Signal Processing*
Objectives: Definition of hardware for number of multiplexing and processing tasks.

Results: On-going.